

PM/96-30
October 1996

**Di-Boson production at Hadron Colliders with
General 3 Gauge Boson Couplings.
Analytic Expressions of Helicity Amplitudes and Cross-Section.**

E. NUSS

Physique Mathématique et Théorique, CNRS-URA 768,
Université de Montpellier II, F-34095 Montpellier Cedex 5.

Abstract

We discuss the tests of general Three Gauge Boson Vertices (TGV) through bosonic pair production at present and future hadron colliders. All bosonic final states are reviewed via the tree level quark-antiquark annihilation sub-process. The full analytic expressions of the helicity amplitudes and cross-sections are given. These expressions should be useful in any attempt to disentangle the effects of the most general non standard WWV ($V = \gamma, Z$) vertices including 14 free parameters. We investigate the sensitivity of the invariant mass and transverse momentum distributions to the full set of anomalous couplings including final state polarization structures. We particularly consider these features at the projected CERN Large Hadron Collider (LHC) energy scale.

arXiv:hep-ph/9610309v1 10 Oct 1996

1. Introduction.

It is well known that in spite of its elegant theoretical construction and a lot of experimental confirmations, the Standard Model (SM) cannot be considered as the final theory of matter and its interactions. As it can be done for the Fermi theory in regard of the SM, it seems reasonable to consider the electroweak theory as the low energy residual part of a more fundamental theory supposed to be found at higher energy scale. It is clear that the crucial point of this hypothesis is to find a direct or indirect signal of this "new" physics (NP). Numerous theoretical studies strongly suggest that NP is to be expected in the TeV range.

The high accuracy of experiments on electroweak measurements at LEP1 and SLC probe the predictions of the SM at few $\times 10^{-3}$ level [1] and do not lead to any undisputable deviation albeit possible deviations in A_b [2]. With the same proviso on the measurement of heavy quarks observables, no departure from the SM is measured up to FERMILAB energy scale [3]. The task of future experiments will be to probe the physics beyond SM. If NP scale is ≥ 1 TeV, it is not certain that future experiments will find it first directly e.g. through the discovery of new interacting particles and we have to look for indirect experimental evidences. As it is briefly reviewed below, the bosonic sector remains poorly tested and, if no Higgs particles is discovered up to the 1 TeV scale, would become one of the most privileged sector for exploring NP like composite W 's, strongly interacting longitudinal W 's or virtual effects of new heavy particles.

At present colliders the process of gauge boson pair production is just below the kinematical limits and the low rate of events leads to very large errors. Given the actual measurements, the bosonic self interactions remain allowed to deviate considerably from their standard expectations but the construction in a near future of a new generation of accelerators will allow us for the first time to make some direct and precise measurements of all three and four boson couplings predicted by the standard electroweak theory. In the SM, these W, Z , and photon self-couplings are strongly related to the scalar sector through the longitudinal components of the vector bosons [4]. Thus, they are an open window on the electroweak gauge symmetry breaking mechanism. They are also a direct manifestation of the non-abelian underlying $SU(2)_L \otimes U(1)_Y$ gauge structure [5] on which the theory is based. In the case of NP related to the mass generation sector, to the gauge symmetry or either to a compositeness of weak-bosons, it is natural to expect that various kinds of anomalous trilinear or quartic couplings will be generated [6]. In the next section we will recall how they can be modeled by some effective anomalous couplings. A direct experimental search for evidence of such anomalous couplings appears clearly as a fundamental test to reach this kind of NP.

As we know, the unitarity of the SM depends directly on its gauge structure. Important cancellations between the amplitudes participating to a process ensure the decrease with energy of the integrated cross-section. Any departure from this vector bosonic gauge structure would break the unitarity at low energy which should lead to an indirect signal of NP. As energy scale is increased, the unitarity should be restored by the contribution of new degrees of freedom.

The main problem is firstly, to test NP existence through the measurement of anomalous couplings. Secondly, we have to characterize this possible NP by an identification of the effective couplings generating those deviations.

Because they are experimentally more accessible and easily treated by effective theories we restrict ourself to the Three Gauge Boson Vertices (TGV) *. Four Gauge Boson Vertices could be related to the previous one in a scenario where the anomalous couplings are generated by the symmetry breakdown of gauge invariant operators [8].

This paper is organized as follows. In Sec.2 we recall some definitions and settle our notations for the general WWV ($V = \gamma, Z$) effective Lagrangian. We briefly link this effective approach to the description of anomalous couplings in term of gauge invariant operators. In Sec.3, we give the explicit expression of the invariant mass and transverse momentum distributions in terms of the usual partonic description used in our numerical computations. In Sec.4, we describe the procedure we apply to obtain the helicity Tables for di-boson production sub-processes which are computed analytically in Sec.5 and 6 for W^+W^- , $W^\pm Z$ and $W^\pm\gamma$ productions. For completeness, we deduce the helicity Tables for the standard ZZ , $Z\gamma$ and $\gamma\gamma$ production from the previous one. We give also the resulting analytic expressions of sub-process cross-section in function of the complete set of anomalous free parameters. In Sec.7, we discuss these results and the implication of the various anomalous couplings to the hadronic observables. We compare standard and non standard shapes of invariant mass and transverse momentum distribution for LHC energy scale. We also give the shapes of the anomalous coupling contributions to the final bosonic polarization states allowed for each productions. Using the fact that the various anomalous couplings contribute to helicity amplitudes in different ways, we suggest a possible procedure to be applied in order to disentangle these couplings.

2. Theoretical Background

In the absence of specific models, the effective Lagrangian approach [9] is extremely useful to parameterize in a model independent way the low-energy effects of NP. We recall that in the approximation of bosons coupled to massless fermions and for on-shell final vector bosons, the most general Lorentz invariant structure for W^+W^-V trilinear vertex †, where $V = Z$ or γ , involves only seven independent terms. This was firstly written in Ref.[11] and reads

$$\begin{aligned} \mathcal{L}_{WWV} = & ie(g_{WWV}^{SM} + \delta_V) \left[V_\mu (W^{\dagger\mu\nu} W_\nu - W^{\mu\nu} W_\nu^\dagger) + V_{\mu\nu} W^\mu W^{\dagger\nu} \right] \\ & + iex_V V^{\mu\nu} W_\mu W_\nu^\dagger + \frac{iey_V}{m_W^2} V^{\nu\lambda} W_{\lambda\mu} W^{\dagger\mu}_\nu \\ & + \frac{ez_V}{m_W^2} (\partial^\alpha \tilde{V}^{\rho\sigma}) \left\{ (\partial_\rho W_\sigma) W_\alpha^\dagger - (\partial_\rho W_\alpha) W_\sigma^\dagger + (\partial_\rho W_\sigma^\dagger) W_\alpha - (\partial_\rho W_\alpha^\dagger) W_\sigma \right\} \end{aligned}$$

*For tests of quartic couplings in colliders experiments, see Ref.[7]

† Analogously to the general WWV vertex it is possible to parameterize anomalous $Z\gamma V$, $V = Z, \gamma$ couplings [10] but these will not be considered here.

$$\begin{aligned}
& + ez'_{1V} \partial^\rho V^\sigma (W_\rho^\dagger W_\sigma + W_\sigma^\dagger W_\rho) + ie z'_{2V} \epsilon^{\mu\nu\rho\sigma} \partial_\mu V_\nu W_\rho^\dagger W_\sigma \\
& + 2ie \frac{z'_{3V}}{m_W^2} \epsilon^{\sigma\rho\alpha\beta} \partial_\sigma V_\mu (\partial^\mu W_\beta \partial_\rho W_\alpha^\dagger + \partial^\mu W_\alpha^\dagger \partial_\rho W_\beta)
\end{aligned} \tag{1}$$

in the notation of Ref.[12]. In Eq.(1), $\epsilon^{0123} = 1$, $V^{\mu\nu} = \partial^\mu V^\nu - \partial^\nu V^\mu$ and $\tilde{V}_{\rho\sigma} = \frac{1}{2}\epsilon_{\rho\sigma\alpha\beta} V^{\alpha\beta}$ denotes the dual field tensor. Higher derivative terms come as form factors of these couplings.

The effective Lagrangian (1) is parameterized in terms of 14 free parameters. For each $V = \gamma$ or Z bosons; $\delta_V, x_V, y_V, z_V, z'_{1V}, z'_{2V}$ and z'_{3V} represent the deviations of the various couplings from their $SU(2)_L \otimes U(1)_Y$ standard values. Electromagnetic gauge invariance fixes to zero δ_γ and z_γ in the limit of on-shell photon ($q^2 = 0$). The tree level standard case corresponds to $g_{WW\gamma}^{SM} = 1$ and $g_{WWZ}^{SM} = \cot \theta_W$ with all anomalous couplings vanishing. The full description of the different couplings and their relations with the equivalent parameterization of Hagiwara et al. [11] can be found in Ref.[12].

In the SM case, all terms of Eq.(1) are generated by perturbative calculations [13]. The MSSM contribution to the x_V and y_V terms, related to the usual magnetic and quadrupole moments κ_V and λ_V through relations $x_V = (\kappa_V - 1)g_V$ and $y_V = \lambda_V g_{WWV}^{SM}$ where $g_V = g_{WWV}^{SM} + \delta_V$, are computed in Ref.[14] and references therein. The minimal effects in the unconstrained MSSM have been found to be of the order of $\Delta\kappa_\gamma = 1 - \kappa_\gamma \simeq 1.75 \cdot 10^{-2}$ and $\Delta\kappa_Z = 1 - \kappa_Z \simeq 0.84 \cdot 10^{-2}$ at LEP II ($\sqrt{s} = 190$ GeV) as compared to a sensitivity of about $5.4 \cdot 10^{-2}$. The λ_V contributions are about a factor 2 – 3 smaller and the SM virtual contributions are of the order of $4.131 \cdot 10^{-3} - 5.505 \cdot 10^{-3}$ for $\Delta\kappa_\gamma$ and $3.323 \cdot 10^{-3} - 3.148 \cdot 10^{-3}$ for $\Delta\kappa_Z$. At NLC ($\sqrt{s} = 500$ GeV), the MSSM effects can reach $\Delta\kappa_V \simeq 5.4 \cdot 10^{-3}$ with a precision of $0.81 \cdot 10^{-3}$. In the general case of non-standard physics, several of these couplings can simultaneously appear, depending on the underlying dynamics [15] and there is no strong theoretical assumptions to privilege any one of them. In this case, the question of finding a strategy to identify and disentangle the effects of the full set of the 14 parameters is raised and will be discussed in Sect.7. Let us discuss, how the non $SU(2)_L \otimes U(1)_Y$ gauge invariant effective Lagrangian (1) can be induced by gauge invariant operators [16, 17]. In this kind of approach, we assume that the NP is invariant under the usual local $SU(2)_L \otimes U(1)_Y$ symmetry and that this symmetry is spontaneously broken by the vacuum expectation value of the Higgs doublet field Φ . Integrating out the heavy degrees of freedom, the interactions between the gauge bosons and the Higgs doublet lead to an effective Lagrangian which describes the residual effects of the full theory at low energy. The full Lagrangian may be written [18]

$$\mathcal{L} = \mathcal{L}_{SM} + \sum_{i,d} \frac{f_i}{\Lambda^{d-4}} O_i^{(d)}(x) \tag{2}$$

where $O_i^{(d)}$ are local operators with mass dimension d greater than four, $SU(2)_L \otimes U(1)_Y$ gauge invariant and involving W, Z, γ and Higgs fields only. The index i runs over all possible operators of a given mass dimension d . Λ denotes the scale at which NP gives a strong contribution in the weak-boson sector. According to Eq.(2) we see that operators of high dimension are suppressed by negative powers of Λ . An exhaustive list of mass-

dimension six operators has been compiled in Ref.[8] and the explicit form of operators generating the full set of TGV's anomalous couplings can be found in Ref.[16].

Several works on TGV study at LEP II through the $e^+e^- \rightarrow W^+W^-$ channel [12, 19] show that despite a relatively clean environment, the weak number of events and the 14 parameters contribution to the same process will not allow to disentangle the different contributions of Eq.(1). However, such an identification is crucial in selecting the operators generating the anomalous couplings. This classification gives fundamental informations on the NP [15] as e.g. an idea of its underlying dynamics, energy scale and a mass bound for its lowest degrees of freedom.

As the unitarity is broken, any deviation from SM couplings leads to amplitudes growing with energy [20, 21], therefore they are more apparent at higher invariant masses of the gauge boson pair but the 200 GeV of LEP II will only allow us to reach the NP scale Λ of Eq.(2) below the $\simeq 2$ TeV range. The future CERN Large Hadron Collider [22] [(LHC), pp collisions at $\sqrt{S} = 14$ TeV] will allow us to explore higher NP scales. Assuming an LHC year of $\int \mathcal{L} dt = 10^5 \text{ pb}^{-1}$ leading to a high rate of production, a detailed study of VV' pair production where $V, V' = W^\pm, Z$ or γ , is particularly interesting to perform TGV measurement and separate their effects.

Hadrons colliders are able to produce gauge boson pairs in both charged and neutral final states but only the W^+W^- , $W^\pm\gamma$ and $W^\pm Z$ channels give a TGV contribution. The first channel suffers from a large QCD background and, as in $e^+e^- \rightarrow W^+W^-$ process, is sensitive to both the $WW\gamma$ and WWZ couplings via the S-channel. In contrast, the $W^\pm\gamma$ and $W^\pm Z$ channels are particularly interesting since they are relatively background free and easy to isolate compared to W^+W^- pair production [23, 24, 25]. These channels are also particularly interesting since they allow independent tests of $WW\gamma$ and WWZ vertices.

The different contributions of the various terms in Eq.(1) to the helicity amplitudes will allow us to disentangle their effects. The best way to distinguish the anomalous couplings is to identify the polarization states of the final bosons for each process which would imply the measurement of angular variables in final leptonic decay.

The $ZZ, Z\gamma$ and $\gamma\gamma$ reactions are not sensitive to the previous TGV but could test the structure functions or a possible non-standard interaction for example related to compositeness of the Z gauge boson (see previous footnote).

While the contribution of any fixed anomalous coupling $\Delta_{g_V}^0$ of Eq.(1) rises without limit as the sub-process energy $\sqrt{\hat{s}}$ increases, eventually violating partial wave unitarity[26], we can choose to parameterize their energetic behavior like a nucleon form factor [21]:

$$\Delta_{g_V}(\hat{s}) = \frac{\Delta_{g_V}^0}{\left(1 + \frac{\hat{s}}{\Lambda_{FF}^2}\right)^n}$$

where Λ_{FF} is a form factor scale depending on the NP scale Λ and is chosen with n as the minimal value compatible with unitarity.

The energy-dependent form factor behavior of anomalous couplings extends the use of effective Lagrangians to the entire energy range which is accessible at hadron colliders

but are based on ad-hoc assumptions by the choice of the values of n and Λ_{FF} . In the case of high production rate, one can suppress these hypotheses on the underlying NP by fitting the couplings assuming they are \hat{s} independent within small energy bins.

3. Partonic Description

We will consider here mainly proton-proton collisions at the LHC energy scale ($\sqrt{S} = 14$ TeV). The results can be easily extended to the $p\bar{p}$ case with appropriate modifications of the structure functions.

The leading lowest-order processes for di-boson production in pp collisions are the boson-boson fusion and the quark-antiquark annihilation illustrated in Fig.1.a and Fig.1.b. In this paper, we will only study the complete case of the Drell-Yann mechanisms of quark annihilation and leave the treatment of boson fusion for a separate analysis [28].

At high energy, these processes are fully described in the partonic approximation [27]. The cross-section $\sigma(pp \rightarrow VV')$ with $V, V' = W^\pm, Z$ or γ is schematically given by [29]

$$d\sigma = \sum_{ij} \int \int dx_a dx_b \{ f_i^{(a)}(x_a) f_j^{(b)}(x_b) + f_j^{(a)}(x_a) f_i^{(b)}(x_b) \} d\hat{\sigma}_{ij} \quad (3)$$

where $f_i^{(a)}$ are the structure functions and contain informations about i -quark luminosity in hadron a . $\hat{\sigma}(q_i \bar{q}'_j \rightarrow VV')$ is the cross-section for the sub-process leading to the desired VV' final state. The x_i and x_j are the momenta fractions of the (i, j) -partons in the nucleons.

The i, j -summation runs over all contributing sea and valence quark configurations and depends on the VV' final state. Neglecting the top quark contribution we write

$(ij) = (u\bar{u}), (d\bar{d}), (s\bar{s}), (c\bar{c}), (b\bar{b})$ for $W^+W^-, Z\gamma, \gamma\gamma$ and ZZ productions;

$(ij) = (u\bar{d}), (c\bar{s})$ for W^+Z or $W^+\gamma$ productions and

$(ij) = (\bar{u}d), (\bar{c}s)$ for W^-Z or $W^-\gamma$ final states.

For $W^\pm Z$ and $W^\pm \gamma$ productions, we neglect the b quark contribution due to the small values of the non-diagonal elements in the Cabibbo-Kobayashi-Maskawa matrix (CKM). Averaging over the quark colors, a common factor of $1/3$ has to be added as well as a statistical factor of $1/2$ in the case of identical final particles ($\gamma\gamma$ and ZZ productions).

Two ingredients are therefore required in order to compute cross-section (3): the sub-process cross-section and the parton distributions. As previously mentioned, a helicity amplitude approach described in Sec.4 will be used to compute the analytic expression of sub-process cross-section. For numerical applications, Martin-Rogerts-Stirling-Distributions(MRSD)' structure functions are used [30] as they best match the recent data from measurements of the proton partonic content.

It is easy to deduce from Eq.(3) the hadronic observable we want to compute. Thanks to the unitarity breaking of anomalous couplings which leads to amplitudes growing with energy, the invariant mass distribution could be a first observable for testing TGV. Indeed, deviations from the SM are more apparent at higher invariant masses of gauge

boson pair by the increase of the number of events which modifies the shape of the invariant mass distribution.

In the $q_i^{(\prime)} \bar{q}_j^{(\prime)} \rightarrow VV' + X$ process, the inclusive differential cross-section for the production of a boson pair such that both intermediate bosons lie in the rapidity interval $(-Y, +Y)$ is given by [31]

$$\frac{d\sigma}{dM} = \frac{2M}{S} \sum_{ij} \int_{-Y}^{+Y} dy_{boost} \left\{ f_i^{(a)}(x_a) f_j^{(b)}(x_b) + f_j^{(a)}(x_a) f_i^{(b)}(x_b) \right\} \int_{-z_0}^{+z_0} dz \frac{d\hat{\sigma}_{ij}}{dz} \quad (4)$$

where $z = \cos \theta$ measures the scattering angle in the parton-parton center of mass (cm). Here, it is convenient to work in terms of the rapidity of a produced vector boson in the hadron-hadron cm frame. The rapidity can be decomposed in $y = y^* + y_{boost}$ where $y^* = \text{Tanh}^{-1}(z\beta_{VV'})$ is the rapidity in the parton-parton center of mass frame. Here, we have defined

$$\beta_{VV'} = \beta \left/ \left(1 + \frac{m^2 - m'^2}{\hat{s}} \right) \right.$$

where m and m' are the masses of the V, V' vectors bosons and the V, V' velocity is

$$\beta = \left[\frac{1}{\hat{s}^2} (\hat{s} + m^2 - m'^2)^2 - \frac{4m^2}{\hat{s}} \right]^{\frac{1}{2}}. \quad (5)$$

The rapidity in the center of mass motion y_{boost} is related to the parton momentum fractions x_a, x_b via the relation $y_{boost} = 1/2 \ln(x_a/x_b)$.

With $\hat{s} = x_a x_b S = M^2$, where M denotes the invariant mass of the vector boson pair and S the pp cm energy, we obtain

$$x_a = \sqrt{\tau} e^{y_{boost}} \quad \text{and} \quad x_b = \sqrt{\tau} e^{-y_{boost}} \quad (6)$$

where $\tau = x_a x_b = \hat{s}/S$.

In our numerical illustrations, we apply an experimental rapidity cut $\pm(Y = 2)$ for the detection of vector bosons which leads to a cut in the parton-parton scattering angle:

$$z_0 = \min \left[\text{Tanh}(Y - |y_{boost}|) / \beta_{VV'}, 1 \right].$$

In the case of a final photon we remove the infrared divergence of the $W\gamma$ pair production cross-section in restricting ourself to the kinematical regions of high $p_{\perp\gamma}$ or invariant mass of the $W^{\pm}\gamma$ pair. This transverse momentum cut p_{cut} leads to

$$z_0 < \left[1 - \frac{p_{cut}^2}{p_{\gamma}^2} \right]^{\frac{1}{2}} \quad \text{with} \quad p_{\gamma} = \frac{\hat{s} - m^2}{2\sqrt{\hat{s}}}.$$

The effects of anomalous couplings are concentrated in the region of small vector boson rapidity since they contribute exclusively to W, Z or photon S-channel exchange. In consequence, the transverse momentum distributions of the vector bosons should be particularly sensitive to the non standard WWV couplings especially for $W^{\pm}Z$ or $W^{\pm}\gamma$ productions which involve only seven anomalous couplings.

The transverse momentum distribution is easily measured by experiment with no ambiguity because only well measured transverse variables are involved. On the contrary, the reconstruction of the invariant mass distribution could be experimentally difficult, due to the unknown longitudinal momentum of the neutrino in the case of a final leptonic decay.

As in the case of the invariant mass distribution, we can express from Eq.(3) the transverse momentum distribution of the vector boson pair production

$$\frac{d\sigma}{dp_{\perp}} = \sum_{ij} \int \int dx_a dx_b \{ f_i^{(a)}(x_a) f_j^{(b)}(x_b) + f_j^{(a)}(x_a) f_i^{(b)}(x_b) \} \frac{d\hat{\sigma}_{ij}}{dp_{\perp}} \quad (7)$$

with $p_{\perp} = |\vec{p}| \sin \theta$ and $p_{\parallel} = |\vec{p}| \cos \theta$. After a Jacobian transformation in (7) we find using relations (6):

$$\frac{d\sigma}{dp_{\perp}} = \frac{1}{S} \sum_{ij} \int \int d\hat{s} dy_{boost} F_{i,j}^{a,b}(\hat{s}, y_{boost}) \frac{d\hat{\sigma}_{ij}}{dp_{\perp}}$$

where

$$F_{i,j}^{a,b}(\hat{s}, y_{boost}) = f_i^{(a)}(\sqrt{\tau}e^{y_{boost}}) f_j^{(b)}(\sqrt{\tau}e^{-y_{boost}}) + f_j^{(a)}(\sqrt{\tau}e^{y_{boost}}) f_i^{(b)}(\sqrt{\tau}e^{-y_{boost}}) .$$

With $\cos \theta = \pm \sqrt{1 - p_{\perp}^2/|\vec{p}|^2}$, the transverse momentum is related to the differential cross-section by

$$\frac{d\hat{\sigma}_{ij}}{dp_{\perp}} = \frac{2p_{\perp}}{\beta\Delta} \frac{d\hat{\sigma}_{ij}}{d\cos \theta}$$

where

$$\Delta = \sqrt{\hat{s}} p_{\parallel} = \frac{1}{2} \sqrt{\hat{s}^2 - 2\hat{s}(m_W^2 + m_{\gamma,Z}^2 + 2p_{\perp}^2) + (m_W^2 - m_{\gamma,Z}^2)^2}$$

gives a Jacobian divergence ($\Delta = 0$) for

$$\hat{s}_{peak} = 2p_{\perp}^2 + m_W^2 + m_{\gamma,Z}^2 + 2\sqrt{(p_{\perp}^2 + m_W^2)(p_{\perp}^2 + m_{\gamma,Z}^2)} .$$

Finally we find the expression of the transverse momentum distribution:

$$\frac{d\sigma}{dp_{\perp}} = \frac{1}{S} \sum_{ij} \int_{\hat{s}_{peak}}^{\hat{s}_{max}} d\hat{s} \int_{-Y}^{+Y} dy_{boost} F_{i,j}^{a,b}(\hat{s}, y_{boost}) \frac{2p_{\perp}}{\beta\Delta} \frac{d\hat{\sigma}_{ij}}{d\cos \theta} . \quad (8)$$

Following relations (4) and (8), both observables could be expressed in terms of the unpolarized differential cross-section. We have to calculate it for the full di-boson production sub-process from quark annihilation:

$$\mathbf{q}_i^{(\prime)} \bar{\mathbf{q}}_i^{(\prime)} \rightarrow \mathbf{W}^+ \mathbf{W}^- , \quad \mathbf{q}_i \bar{\mathbf{q}}_j^{\prime} \rightarrow \mathbf{W}^{\pm} \mathbf{Z} , \quad \mathbf{q}_i \bar{\mathbf{q}}_j^{\prime} \rightarrow \mathbf{W}^{\pm} \gamma$$

and

$$\mathbf{q}_i^{(\prime)} \bar{\mathbf{q}}_i^{(\prime)} \rightarrow \mathbf{Z} \mathbf{Z} , \quad \mathbf{q}_i^{(\prime)} \bar{\mathbf{q}}_i^{(\prime)} \rightarrow \mathbf{Z} \gamma , \quad \mathbf{q}_i^{(\prime)} \bar{\mathbf{q}}_i^{(\prime)} \rightarrow \gamma \gamma .$$

From Eq.(1), it is straightforward to calculate the explicit expression of the helicity amplitudes, at least at low orders in perturbation theory from which the unpolarized differential cross-section will be easily analytically derived.

4. Description in term of the Helicity Amplitudes for Sub-Process study

At this level, it is convenient to fix some kinematical notations for the two-body parton scattering with massless incoming particles.

For the generic process $\mathbf{q}^{(\prime)}(\mathbf{k})\bar{\mathbf{q}}^{(\prime)}(\mathbf{k}') \rightarrow \mathbf{V}(\mathbf{p})\mathbf{V}'(\mathbf{p}')$ where k, k', p, p' denote the 4-momenta, we have in the VV' cm momentum $|\vec{p}| = |\vec{p}'| = \beta\sqrt{s}/2$ where β is given in Eq.(5). The s, t, u variables represent the usual Mandelstam variables with $s + t + u = m^2 + m'^2$. Following the procedure given in Ref.[32], we will decompose the amplitudes in the chirality-conserving invariant form $(N_i, i = 1, \dots, 9)$ helicity basis

$$\begin{aligned} N_1 &= \not{\epsilon}'\epsilon.k' & N_2 &= \not{\epsilon}'\epsilon.k & N_3 &= \not{\epsilon}\epsilon'.k' \\ N_4 &= \not{\epsilon}\epsilon'.k & N_5 &= \not{p}\epsilon.\epsilon' & N_6 &= \not{p}'\epsilon'.k'\epsilon.k \\ N_7 &= \not{p}'\epsilon'.k\epsilon.k' & N_8 &= \not{p}'\epsilon'.k\epsilon.k & N_9 &= \not{p}'\epsilon'.k'\epsilon.k' . \end{aligned} \quad (9)$$

ϵ and ϵ' are the polarization vectors of the final bosons and could be written in the cm frame as [33]

$$\left\{ \begin{aligned} \epsilon^\mu(p, \tau = \pm 1) &= \frac{e^{-i\tau\varphi}}{\sqrt{2}} [0, -\tau \cos \theta \cos \varphi - i \sin \varphi, -\tau \cos \theta \sin \varphi + i \cos \varphi, \tau \sin \theta] \\ \epsilon^\mu(p, 0) &= \left[\frac{|\vec{p}|}{m}, \frac{1}{m}e \sin \theta \cos \varphi, \frac{1}{m}e \sin \theta \sin \varphi, \frac{1}{m}e \cos \theta \right] \end{aligned} \right.$$

and

$$\left\{ \begin{aligned} \epsilon'^\mu(p', \tau' = \pm 1) &= \frac{e^{+i\tau'\varphi}}{\sqrt{2}} [0, \tau' \cos \theta \cos \varphi - i \sin \varphi, \tau' \cos \theta \sin \varphi + i \cos \varphi, -\tau' \sin \theta] \\ \epsilon'^\mu(p', 0) &= \left[\frac{-|\vec{p}'|}{m'}, \frac{1}{m'}e' \sin \theta \cos \varphi, \frac{1}{m'}e' \sin \theta \sin \varphi, \frac{1}{m'}e' \cos \theta \right] \end{aligned} \right.$$

where

$$e = \frac{1}{2\sqrt{s}}(s + m^2 - m'^2) \quad \text{and} \quad e' = \frac{1}{2\sqrt{s}}(s + m'^2 - m^2) .$$

θ denotes the scattering angle measured in the VV' rest frame between the incident quark momentum \vec{k} and the final V boson momentum \vec{p} . The angle φ denotes the azimuthal angle and $\tau, \tau' = \pm 1, 0$ are the polarizations of the final V and V' bosons. Suggested by the procedure given in Ref.[12], all the invariant amplitudes could be decomposed on (9) as

$$R = \sum_j c_j \bar{v}(k') N_j (a - b\gamma^5) u(k) . \quad (10)$$

where a and b stand for the general vector and axial vector couplings.

The 9 helicity amplitudes for each process $q(\lambda)\bar{q}'(\lambda') \rightarrow V(\tau)V'(\tau')$, where $\lambda = -\lambda' = \pm 1/2$ denotes the quark helicities, are then directly obtained from the helicity decomposition of the N_i 's. They may be written as

$$F_{\lambda\lambda'\tau\tau'}(s, \theta, \varphi) = \sum_j c_j F_{\lambda\lambda'\tau\tau'}(N_j, s, \theta, \varphi)(a - 2b\lambda) \quad (11)$$

with

$$F_{\lambda\lambda'\tau\tau'}(N_j, s, \theta, \varphi) = e^{i(\lambda-\lambda')\varphi} f_{\lambda\lambda'\tau\tau'}(N_j, s, \theta)$$

where

$$f_{\lambda\lambda'\tau\tau'}(N_j, s, \theta) = \frac{s\lambda'}{2} \mathcal{N}_j \delta_{\lambda, -\lambda'} .$$

The expression of the \mathcal{N}_i 's are given in Table 1.

For each process, the helicity amplitudes will be calculated in the next section and are displayed in Tables 2, 3, 4 and 5 with the following generic notations for the VV' helicity Tables:

| | | | | | | |
|-------|----------------|------------------------|-------------------------|--------------------|---------------------------|---------------------------|
| | | $\tau = \tau' = \pm 1$ | $\tau = -\tau' = \pm 1$ | $\tau = \tau' = 0$ | $\tau = 0, \tau' = \pm 1$ | $\tau = \pm 1, \tau' = 0$ |
| | $\alpha_{VV'}$ | Θ_1 | Θ_2 | Θ_3 | Θ_4 | Θ_5 |
| ξ | Γ_ξ | $\Psi_{\xi,1}$ | $\Psi_{\xi,2}$ | $\Psi_{\xi,3}$ | $\Psi_{\xi,4}$ | $\Psi_{\xi,5}$ |

where ξ runs in a column over the lines denoted $T, U, G, X, Y, Z, Z'_1, Z'_2$ and Z'_3 .

To obtain the amplitude $F_{\lambda\lambda'\tau\tau'}$ for definite quark helicity $\lambda = \pm 1/2$, each element $\Psi_{\xi,n}$ of a line ξ and column n corresponding to a definite polarization $\tau(V)$ and $\tau'(V')$ of the bosons has to be multiplied by the common factor Θ_n on top of the column and its corresponding elements Γ_ξ in the second column. The sum over all elements (i.e. over ξ) and the global factor $\alpha_{VV'}$ is to be taken. This rule is applied for each particular final state VV' ($W^+W^-, W^\pm Z, W^\pm \gamma$ or $ZZ, Z\gamma, \gamma\gamma$) to the corresponding helicity Tables 2, 3, 4 and 5:

$$F_{\lambda\lambda'\tau\tau'} = \alpha_{VV'} \Theta_n \sum_\xi \Gamma_\xi \Psi_{\xi,n} .$$

Afterwards, it is easy to compute the expression of the differential cross-section in terms of helicity amplitude products. It reads [‡]

$$\frac{d\sigma}{d\cos\theta} = \frac{|\vec{p}'|}{16\pi s\sqrt{s}} \sum_{\lambda\lambda'\tau\tau'} |F_{\lambda\lambda'\tau\tau'}|^2 = \frac{|\vec{p}'|}{16\pi s\sqrt{s}} \alpha_{VV'}^2 \sum_{n=1}^5 \sum_{\lambda\lambda'} |\Theta_n \sum_\xi \Gamma_\xi \Psi_{\xi,n}|^2 . \quad (12)$$

Each cross-section could also be expressed in the form

$$\frac{d\sigma}{d\cos\theta} = C \sum_{i=1}^N \mathcal{O}_{VV'}^{\xi, \xi'}(i) \mathcal{F}_{VV'}^{\xi, \xi'}(i) \quad (13)$$

[‡] Bosonic states have been normalized as $\langle p'|p \rangle = (2\pi)^3 2E\delta(\vec{p} - \vec{p}')$ while the quark states are normalized as $\langle p'|p \rangle = (2\pi)^3 \frac{E}{m_q} \delta(\vec{p} - \vec{p}')$.

where $C = (\pi\alpha^2|\vec{p}'|)/(4s\sqrt{s})$ and $\alpha = e^2/4\pi$. ξ and $\xi' = T, U, G, X, Y, Z, Z'_1, Z'_2$ or Z'_3 and stand for the interferences of the various terms in the amplitude products. In Eq.(13), all the $\mathcal{O}_{VV'}^{\xi;\xi'}(i)$ are purely kinematical coefficients and the $\mathcal{F}_{VV'}^{\xi;\xi'}(i)$ are combinations of coupling constants depending on the anomalous three boson coupling parameters. Integrating analytically the $\mathcal{O}_{VV'}^{\xi;\xi'}(i)$ between $-z_0$ and z_0 it is easy to compute the integrated cross-section to obtain the invariant mass distribution of Eq.(4).

The $\mathcal{O}_{VV'}^{\xi;\xi'}(i)$ and the $\mathcal{F}_{VV'}^{\xi;\xi'}(i)$ depend strongly on the final bosonic state and will be given below for each process. We divide them into three sets, the first set which already exists in the standard case, the second set deals with couplings conserving CP and the last set appears only through CP -violating ones. Both formulations of the cross-section in Eq.(12) and Eq.(13) give two different numerical calculations tools and allow for various cross-checks.

5. $q_i^{(\prime)}\bar{q}_i^{(\prime)} \rightarrow W^+W^-$ process

The three lowest order Feynman diagrams for W^+W^- gauge boson pair production from the $q^{(\prime)}\bar{q}^{(\prime)}$ annihilation are shown in Fig.2 and are very similar to the $e^+e^- \rightarrow W^+W^-$ contributions. The U- and T-channels correspond respectively to the up or down quark-antiquark annihilation. The S-channel induces a sensitivity to both $WW\gamma$ and WWZ couplings.

The quark exchange part in the T-channel is written as

$$R_{WW}(t) = -\frac{e^2}{t}\bar{v}(k')\not{\epsilon}'(\not{k} - \not{p})\not{\epsilon}a_T(1 - \gamma^5)u(k)$$

where $a_T = 2a_{Wii}^2$ correspond to the general vector and axial vector couplings a_{Wij} and b_{Wij} for $q_i\bar{q}_j'W^\pm$ vertex:

$$a_{Wij} = b_{Wij} = \frac{1}{2\sqrt{2}\sin\theta_W}V_{ij} .$$

V_{ij} are the elements of the CKM quark mixing matrix and θ_W the weak mixing angle of Weinberg.

According to Eq.(10), the decomposition on the helicity basis (9) gives

$$\begin{aligned} R_{WW}(t) &= -\frac{e^2}{st}\bar{v}(k')\left\{(s + m_W^2 - t)(N_2 - N_3) + (m_W^2 - t)(N_1 - N_4)\right. \\ &\quad \left.+ sN_5 + 2(N_7 - N_6)\right\}a_T(1 - \gamma^5)u(k) . \end{aligned} \quad (14)$$

In the same way the U-channel is written as

$$\begin{aligned} R_{WW}(u) &= -\frac{e^2}{u}\bar{v}(k')\not{\epsilon}(\not{k} - \not{p}')\not{\epsilon}'a_U(1 - \gamma^5)u(k) \\ &= -\frac{e^2}{su}\bar{v}(k')\left\{(s + m_W^2 - u)(N_4 - N_1) + (m_W^2 - u)(N_3 - N_2)\right. \\ &\quad \left.- sN_5 + 2(N_7 - N_6)\right\}a_U(1 - \gamma^5)u(k) \end{aligned} \quad (15)$$

with $a_U = a_T$. For the contribution of the S-channel, we use the notations of Fig.3. It is straightforward to derive the Feynman rules for the three-boson vertices in W^+W^- production from the phenomenological effective Lagrangian (1):

$$\begin{aligned}
\mathcal{V}_\mu^V &= g_V[\epsilon.\epsilon'(p-p')_\mu - 2\epsilon'.p\epsilon_\mu + 2\epsilon.p'\epsilon'_\mu] + x_V[\epsilon.p'\epsilon'_\mu - \epsilon'.p\epsilon_\mu] \\
&+ \frac{y_V}{m_W^2}[q_\nu g_{\lambda\mu} - q_\lambda g_{\nu\mu}][p'^\lambda\epsilon'^\rho - p'^\rho\epsilon'^\lambda][p_\rho\epsilon^\nu - p^\nu\epsilon_\rho] \\
&+ i\frac{z_V}{m_W^2}\epsilon_{\mu\nu\rho\sigma}q^\nu(p'-p)^\rho[\epsilon'.p\epsilon^\sigma - \epsilon.p'\epsilon'^\sigma] + iz'_{1V}[\epsilon'.p\epsilon_\mu + \epsilon.p'\epsilon'_\mu] \\
&+ z'_{2V}\epsilon_{\mu\nu\rho\sigma}q^\nu\epsilon^\rho\epsilon'^\sigma - \frac{z'_{3V}}{m_W^2}(p'-p)_\mu\epsilon_{\tau\nu\rho\sigma}q^\tau(p'-p)^\nu\epsilon^\rho\epsilon'^\sigma. \tag{16}
\end{aligned}$$

The two amplitudes in the S-channel ($V = \gamma$ or Z) are

$$R_{WW}^V(s) = \frac{e^2}{D_V(s)}\bar{v}(k')\gamma^\mu(a_{Vi} - b_{Vi}\gamma^5)u(k)\mathcal{V}_\mu^V$$

where $D_\gamma(s) = s$ and, in the $s > 4m_Z^2$ case, the Z propagators is approximated to $D_Z(s) \simeq s - m_Z^2$.

The vector boson- $q\bar{q}$ couplings a_{Vi} and b_{Vi} are kept in standard forms: for $q_i q'_i \gamma$ vertex

$$a_{\gamma i} = Q_i, \quad b_{\gamma i} = 0$$

and for $q_i q'_i Z$ vertex

$$a_{Zi} = \frac{1}{4\sin\theta_W\cos\theta_W}(\tau_3^i - 4Q_i\sin^2\theta_W), \quad b_{Zi} = \frac{1}{4\sin\theta_W\cos\theta_W}\tau_3^i$$

where Q_i and τ_3^i are the electric charge and weak isospin projection of the i -quark:

$$\begin{cases} Q_i = 2/3, \tau_3^i = 1 \text{ for up quark} \\ Q_i = -1/3, \tau_3^i = -1 \text{ for down quark.} \end{cases}$$

Following Ref.[12], the decomposition of Eq.(16) on helicity basis (9) leads to:

$$\begin{aligned}
R_{WW}^V(s) &= \frac{e^2}{D_V(s)}\bar{v}(k')\left\{2g_V(N_1 + N_2 - N_3 - N_4 + N_5) \right. \\
&+ x_V(N_1 + N_2 - N_3 - N_4) \\
&+ \frac{y_V}{m_W^2}\left[sN_5 + m_W^2(N_1 + N_2 - N_3 - N_4) \right. \\
&\quad \left. + 2(N_6 + N_7 + N_8 + N_9)\right] \\
&- \frac{z_V}{m_W^2}\left[(t-u)(N_1 + N_2 - N_3 - N_4) + 4(N_6 - N_7)\right]\gamma^5 \\
&+ iz'_{1V}(N_1 + N_2 + N_3 + N_4) + iz'_{2V}(N_1 + N_4 - N_2 - N_3)\gamma^5 \\
&- i\frac{z'_{3V}}{m_W^2}\left[(s - 4m_W^2)(N_1 - N_2 - N_3 + N_4) - 2(t - m_W^2 + \frac{s}{2}) \times \right. \\
&\quad \left.(N_1 + N_2 + N_3 + N_4) + 4(N_8 - N_9)\right]\gamma^5\left\}(a_{Vi} - b_{Vi}\gamma^5)u(k). \tag{17}
\end{aligned}$$

According to the procedure given in Sec.4 and to Eq.(11), the Eq.(14), (15) and (17) lead to the helicity Table 2 for $\mathbf{q}_i^{(\prime)} \bar{\mathbf{q}}_i^{(\prime)} \rightarrow \mathbf{W}^+ \mathbf{W}^-$.

Defining for convenience $\chi_Z = s/(s - m_Z^2)$, $a_Z = a_{Zi}$, $b_Z = b_{Zi}$, $a_T = a_U = 2a_{Wij}^2$ and the intermediate functions as follows:

$$\begin{aligned}
\mathcal{G}_{WW}^{V,V}(c_\gamma, c'_\gamma, c_Z, c'_Z) &= c_\gamma c'_\gamma a_\gamma^2 + c_Z c'_Z (a_Z^2 + b_Z^2) \chi_Z^2 \\
&\quad + (c_\gamma c'_Z + c_Z c'_\gamma) a_\gamma a_Z \chi_Z \\
\mathcal{G}_{WW}^{V,(T \text{ or } U)}(c_\gamma, c_Z) &= a_T [a_\gamma c_\gamma + (a_Z + b_Z) \chi_Z c_Z] \\
\mathcal{G}_{WW}^{Z,Z} &= z_\gamma^2 a_\gamma^2 + z_Z^2 (a_Z^2 + b_Z^2) \chi_Z^2 + 2z_\gamma z_Z a_\gamma a_Z \chi_Z \\
\mathcal{G}_{WW}^{GXY,Z} &= a_\gamma b_Z \chi_Z [z_\gamma (2g_Z + x_Z + y_Z) + z_Z (2g_\gamma + x_\gamma + y_\gamma)] \\
&\quad + 2a_Z b_Z \chi_Z^2 z_Z (2g_Z + x_Z + y_Z) \\
\mathcal{G}_{WW}^{Z,(T \text{ or } U)} &= -a_T [a_\gamma z_\gamma + (a_Z + b_Z) \chi_Z z_Z]
\end{aligned}$$

we find with the help of helicity Table 2 the expressions of the $\mathcal{F}_{WW}^{\xi, \xi'}(i)$ and $\mathcal{O}_{WW}^{\xi, \xi'}(i)$ terms of Eq.(13) for $\mathbf{q}_i^{(\prime)} \bar{\mathbf{q}}_i^{(\prime)} \rightarrow \mathbf{W}^+ \mathbf{W}^-$.

These terms are summarized in Tables 6, 7 and 8.

6. $\mathbf{q}_i \bar{\mathbf{q}}_j' \rightarrow \mathbf{W}^\pm \mathbf{Z}$ and $\mathbf{q}_i \bar{\mathbf{q}}_j' \rightarrow \mathbf{W}^\pm \gamma$ processes

The three lowest order Feynman diagrams for $W^\pm V$, $V = \gamma, Z$ production from $q\bar{q}'$ annihilation are shown in Fig.4.

For $W^+ V$ production, the T-channel amplitude is

$$R_{W^+V}(t) = -\frac{e^2}{t} \bar{v}(k') \not{\epsilon}' (\not{k} - \not{p}) \not{\epsilon} a_T (1 - \gamma^5) u(k)$$

with $a_T = a_{Wij}(a_{Vj} + b_{Vj})$. The decomposition on the helicity basis (9) gives

$$\begin{aligned}
R_{W^+V}(t) &= -\frac{e^2}{st} \bar{v}(k') \left\{ -(s + m_V^2 - t) N_3 + (s + m_W^2 - t) N_2 + (m_V^2 - t) N_1 \right. \\
&\quad \left. - (m_W^2 - t) N_4 + s N_5 + 2(N_7 - N_6) \right\} a_T (1 - \gamma^5) u(k) .
\end{aligned} \tag{18}$$

In the same way, the contribution of the U-channel amplitude is

$$R_{W^+V}(u) = -\frac{e^2}{u} \bar{v}(k') \not{\epsilon} (\not{k} - \not{p}') \not{\epsilon}' a_U (1 - \gamma^5) u(k)$$

with $a_U = a_{Wij}(a_{Vi} + b_{Vi})$ and leads through (9) to

$$\begin{aligned}
R_{W^+V}(u) &= -\frac{e^2}{su} \bar{v}(k') \left\{ (s + m_V^2 - u) N_4 - (s + m_W^2 - u) N_1 + (m_W^2 - u) N_3 \right. \\
&\quad \left. - (m_V^2 - u) N_2 - s N_5 + 2(N_7 - N_6) \right\} a_U (1 - \gamma^5) u(k) .
\end{aligned} \tag{19}$$

With the notations of Fig.5, we derive the Feynman rules for the $W^\pm(Z, \gamma)$ production with the complete TGV contribution of Lagrangian (1):

$$\begin{aligned}
\mathcal{V}_\mu^V &= \eta g_V \left[\epsilon \cdot \epsilon' (p - p')_\mu - 2\epsilon' \cdot p \epsilon_\mu + 2\epsilon \cdot p' \epsilon'_\mu \right] + \eta x_V \left[\epsilon \cdot \epsilon' p_\mu - \epsilon' \cdot p \epsilon_\mu \right] \\
&\quad - \eta \frac{y_V}{m_W^2} \left[\epsilon \cdot p' \epsilon' \cdot p (p - p')_\mu - p^2 \epsilon \cdot p' \epsilon'_\mu + p'^2 \epsilon' \cdot p \epsilon_\mu - \epsilon \cdot \epsilon' p' \cdot q p_\mu + \epsilon \cdot \epsilon' p \cdot q p'_\mu \right] \\
&\quad - i \frac{z_V}{m_W^2} \epsilon_{\rho\sigma\alpha\beta} p^\alpha \epsilon'^\beta (2p' + p)^\rho (\epsilon' \cdot p g^{\mu\sigma} - \epsilon'^\sigma p^\mu) \\
&\quad - i z'_{1V} \left[\epsilon \cdot \epsilon' p_\mu + \epsilon' \cdot p \epsilon_\mu \right] - \eta z'_{2V} \epsilon_{\mu\nu\rho\sigma} p^\rho \epsilon'^\sigma \epsilon'^\nu \\
&\quad - \eta \frac{z'_{3V}}{m_W^2} \epsilon_{\mu\nu\rho\sigma} p^\rho \epsilon'^\nu (2p' + p)^\sigma \epsilon \cdot p'
\end{aligned}$$

where $\eta = \mp 1$ for a W^\pm in the final state.

The W^+ formation part is given by

$$R_{W^+V}(s) = \frac{e^2}{D_W(s)} \bar{v}(k') \gamma^\mu (a_{Wij} - b_{Wij} \gamma^5) u(k) \mathcal{V}_\mu^V \quad (20)$$

where the W propagator is approximated as $D_W(s) \simeq s - m_W^2$.

The decomposition of Eq.(20) on the helicity basis (9) gives

$$\begin{aligned}
R_{W^+V}(s) &= \frac{e^2}{D_W(s)} \bar{v}(k') \left\{ -2g_V(N_1 + N_2 - N_3 - N_4 + N_5) \right. \\
&\quad - x_V(N_5 - N_3 - N_4) \\
&\quad - \frac{y_V}{m_W^2} \left[sN_5 + m_V^2(N_1 + N_2) - m_W^2(N_3 + N_4) \right. \\
&\quad \left. \left. + 2(N_6 + N_7 + N_8 + N_9) \right] \right. \\
&\quad + \frac{2z_V}{sm_W^2} \left[(N_6 - N_7)(s + m_V^2 - m_W^2) - \frac{s^2\beta^2}{4}(N_1 - N_2 + N_4 - N_3) \right. \\
&\quad \left. + \frac{1}{4}s\beta \cos\theta (s + m_V^2 - m_W^2)(N_1 + N_2 - N_3 - N_4) \right] \gamma^5 \\
&\quad - iz'_{1V}(N_3 + N_4 + N_5) \\
&\quad + iz'_{2V} \left[\frac{1}{2s}(s + m_V^2 - m_W^2)(N_1 - N_2 - N_3 + N_4) \right. \\
&\quad \left. - \frac{1}{2}\beta \cos\theta (N_1 + N_2 - N_3 - N_4) - \frac{2}{s}(N_6 - N_7) \right] \gamma^5 \\
&\quad + i \frac{z'_{3V}}{m_W^2} \left[4(N_8 - N_6 + N_7 - N_9) \right. \\
&\quad \left. - 2s\beta \cos\theta (N_1 + N_2) \right] \gamma^5 \left. \right\} a_{Wij} (1 - \gamma^5) u(k) . \quad (21)
\end{aligned}$$

Eq.(18), (19) and (21) are similar for W^-V production and according to the procedure given in Sec.4 and to Eq.(11), lead to the helicity Table 3 for $W^\pm Z$ final state and Table 4 for $W^\pm \gamma$ final state.

As before, we can find the expressions of the $\mathcal{F}_{W(Z \text{ or } \gamma)}^{\xi, \xi'}(i)$ and $\mathcal{O}_{W(Z \text{ or } \gamma)}^{\xi, \xi'}(i)$ terms of Eq.(13) for $\mathbf{q}_i \bar{\mathbf{q}}'_j \rightarrow \mathbf{W}^\pm \mathbf{Z}$ and $\mathbf{q}_i \bar{\mathbf{q}}'_j \rightarrow \mathbf{W}^\pm \gamma$ with respectively the helicity Tables 3 and 4.

Defining for $W^\pm Z$ and $W^\pm \gamma$ productions $\chi_W = 1/(s - m_W^2)$ and the intermediate functions as follows:

$$\begin{aligned}
\mathcal{G}_{WV}^{V,V}(c, c') &= cc' a_{Wij}^2 \chi_W^2 \\
\mathcal{G}_{WV}^{V,T}(c) &= a_{Wij}^2 (a_{Vj} + b_{Vj}) \chi_W c \\
\mathcal{G}_{WV}^{V,U}(c) &= a_{Wij}^2 (a_{Vi} + b_{Vi}) \chi_W c \\
\mathcal{G}_{WV}^{GXY,Z} &= -a_{Wij}^2 \chi_W^2 z_V (2g_V + x_V + y_V) \\
\mathcal{G}_{WV}^{Z,T} &= -a_{Wij}^2 (a_{Vj} + b_{Vj}) \chi_W z_V \\
\mathcal{G}_{WV}^{Z,U} &= -a_{Wij}^2 (a_{Vi} + b_{Vi}) \chi_W z_V \\
\mathcal{G}_{WV}^{Z,Z} &= \mathcal{G}_{WV}^{VV}(z_V, z_V) \\
\mathcal{G}_{WV}^{T,T} &= a_{Wij}^2 (a_{Vj} + b_{Vj})^2 \\
\mathcal{G}_{WV}^{U,U} &= a_{Wij}^2 (a_{Vi} + b_{Vi})^2 \\
\mathcal{G}_{WV}^{T,U} &= a_{Wij}^2 (a_{Vi} + b_{Vi})(a_{Vj} + b_{Vj})
\end{aligned}$$

we find the results of Table 9 for the $\mathcal{F}_{WV}^{\xi, \xi'}(i)$ where $V = Z$ or γ . The kinematical variables $\mathcal{O}_{WV}^{\xi, \xi'}(i)$ are summarized in Tables 10 and 11 for $W^\pm Z$ production and in Tables 12 and 13 for $W^\pm \gamma$ production.

7. Discussion

As previously mentioned, in the most general case we have to deal with seven $WW\gamma$ and seven WWZ couplings. When we allow for more than one anomalous coupling to be non zero it is clear that the possibilities of correlations can not be excluded. The question of making a significant test of the SM involves three steps: 1) measuring independently and precisely each WWV vertex; 2) checking whether they agree with the SM values; 3) possibly, disentangling the effects of the various anomalous couplings.

Eq.(2) leads generally to a $(\sqrt{\hat{s}}/\Lambda)^{d-4}$ energetic behavior [15]. For an expected value of the NP scale Λ in the TeV range, it seems obvious that one does not expect a violent low energy departure from the standard predictions, i.e. the 14 parameters $\delta_V, x_V, y_V, z_V, z'_{1V}, z'_{2V}$ and z'_{3V} ($V = \gamma, Z$) should have reasonably small values. Nevertheless, for large values of the di-boson invariant mass $\sqrt{\hat{s}}$ and provided that the signal is not overwhelmed by the background, the non-standard contributions to the helicity amplitudes would dominate. Information on anomalous WWV couplings should be obtained in comparing the shapes of the measured and predicted transverse momenta or invariant mass distributions for each $W^\pm V$, ($V = W^\pm, Z, \gamma$) productions. As suggested in Ref.[23] and [34], the uncertainty on the structure functions should be reduced by considering ratios of non-standard and standard contributions as for example:

$$\frac{\sigma(pp \rightarrow W^\pm Z) Br(W^\pm \rightarrow l^\pm \nu) Br(Z \rightarrow l^+ l^-)}{\sigma(pp \rightarrow ZZ) Br(Z \rightarrow l^+ l^-)^2} .$$

The presence of anomalous couplings in the WWV vertex will yield an enhanced number of events at large invariant mass M_{WV} or $p_{\perp V}$ transverse momentum of the $W^\pm V$ system. As an illustration, the sensitivity of the various distributions to deviations from standard couplings has been tested by changing the parameters from their SM expectations. The resulting shapes are displayed for $V = \gamma, Z$ and for several choices of anomalous couplings in Fig.6 and Fig.7. The leptonic branching ratios per lepton species are included in the cross-section and have been taken to be $Br(W^\pm Z \rightarrow l_1^\pm \nu_1 l_2^\pm l_2^-) = 0.36\%$ and $Br(W^\pm \gamma \rightarrow l_{1,2}^\pm \nu_{1,2} \gamma) = 10.7\%$ with $l_{1,2}^\pm = e^\pm$ or μ^\pm . Note that around 300 GeV for $p_{\perp Z}$ and 150 GeV for $p_{\perp \gamma}$, one can get an effect between 5 and 50 % even for moderate values of the anomalous couplings. Of course, for the same values of the couplings, higher effects can be reach at higher $p_{\perp(Z,\gamma)}$.

Here, as a starting point, we do not allow for several parameters to be simultaneously non vanishing and only one coupling is assumed to deviate from the SM at a time.

In practice, large cancellations between the different terms cannot be excluded and the full set of parameters have to be considerate simultaneously. In this case, the limits of observability for the couplings will be obtained by a multi-parameter analysis. To perform this analysis, we can use a Maximum Likelihood fit [35] or methods based on density matrix or optimal observables respectively exposed in Ref.[12] and [36]. The helicity Tables 2,3,4 and the analytic expressions of Tables 6 to 13 will be useful to perform this analysis which has to be done in a phase space region where the effects of non standard Three Vector Boson Couplings are much larger than the background.

For completeness, we deduce the helicity amplitudes of the standard ZZ , $Z\gamma$ and $\gamma\gamma$ productions from the previous W^+W^- and $W^\pm V$ cases. We reproduce them in Table 5. Only the T- and U-channels are allowed in our scenario and using the same notations as for the other productions, they lead to the $\mathcal{O}_{VV'}^{\xi,\xi'}(i)$ and $\mathcal{F}_{VV'}^{\xi,\xi'}(i)$ expressions of Table 14 (with $VV' = ZZ$, $Z\gamma$ or $\gamma\gamma$).

Now, we would like to show why, starting from the most general case of 14 free parameters, one can in principle construct a strategy for disentangling the parameters if one identifies the Longitudinal(L) or Transverse(T) polarization states of the final W^\pm and V bosons.

In what follows, we shall discuss the contributions of anomalous couplings to the helicity amplitudes. The helicity Table 2 corresponding to W^+W^- production having an identical structure to the one done for the $e^+e^- \rightarrow W^+W^-$ process, the reader is referred to Ref.[12] and [19] for extensive discussion. A glance at the helicity amplitudes of Tables 3 and 4 allows us immediately to draw several useful conclusions on the contributions of the various couplings to the $W^\pm Z$ and $W^\pm \gamma$ final states.

For $W^\pm Z$ production, the helicity amplitudes lead to strong mixing among the three types of C- and P-conserving forms corresponding to the δ_Z , x_Z and y_Z couplings (i.e. the deviation of Yang-Mills coupling, the magnetic and the quadrupole terms). However,

these three forms contribute, like the CP-conserving but C- and P- violating coupling z_Z and like the three other CP-violating couplings z'_{1Z} , z'_{2Z} and z'_{3Z} , to the final polarization states (TT , LL and LT) with very different weights. Thus, the measurement of the vector boson polarization (spin density matrix elements) will be crucial for separating their effects. More precisely, as shown in Table 3, one observes that δ_Z , x_Z , and z'_{1Z} contribute to all of the TT , LL and LT state while y_Z , z_Z , z'_{2Z} and z'_{3Z} contribute to TT and LT but not to LL state. Similarly to W^+W^- production, there is no TT contribution coming from the S-channel in the case of opposite polarization, $\tau = -\tau' = \pm 1$.

The standard and all anomalous contributions to the Z transverse momentum distribution with TT, LL or LT final $W^\pm Z$ polarization states are shown in Fig.8. Due to the same dependence in the $q\bar{q}$ sub-process, an identical behavior can be observed in the shapes of the invariant mass distribution of the $W^\pm Z$ pair. For conciseness, these shapes are not included in this study and are postponed in a forthcoming paper.

According to the helicity Table 3, we observe in Fig.8.b that for the δ_Z coupling, the high energy behavior is dominated by TT and LL productions whereas, as shown in Fig.8.c, the x_Z coupling contribute essentially to TT and LT productions. The amplitudes corresponding to y_Z (see Fig.8.d) and z'_{1Z} (see Fig.8.f) couplings are respectively dominated by TT and LL productions. Furthermore, the z_Z , z'_{2Z} and z'_{3Z} couplings contribute essentially to LT final state but with different energy dependence for this production (Fig.8.e, Fig.8.g and Fig.8.h).

All those properties should allow a clear separation between all the different WWZ anomalous couplings.

The $W^\pm\gamma$ final state leads to helicity amplitudes very similar to the previous $W^\pm Z$ process except for the z'_{3V} contribution which vanishes in $W^\pm\gamma$ production. In Fig.9.a, 9.b, 9.c and 9.d, we show respectively the SM and the x_γ , y_γ , z_γ contributions to the photon transverse momentum distribution with TT or LT final $W^\pm\gamma$ polarization states. As in the $W^\pm Z$ case, one observes the same behavior between the invariant mass distribution and the photon transverse momentum distribution for all allowed final polarizations. Helicity Table 4 shows that the δ_γ and x_γ couplings have the same contribution. Their high energy behavior is dominated by the $1/m_W\sqrt{s}$ term of the LT state as for $z'_{1\gamma}$ and $z'_{2\gamma}$ couplings (see Fig.9.b). Thus, there is no possibility to disentangle any of these couplings through their effect in $W^\pm\gamma$ production only. A complete separation of the effects for these $WW\gamma$ anomalous couplings needs an additional analysis. Using a multiparameter fit, we can study for example the interplay between different anomalous couplings being simultaneously non-zero in $W^\pm\gamma$ production. We can also test the W^+W^- production which is sensitive to both WWZ and $WW\gamma$ anomalous couplings and where the previous contributions are not identical.

The y_γ and the anapole coupling z_γ can be separated from the others as the TT state has a strong increase with \sqrt{s} for y_γ (Fig.9.c), while the contribution of the z_γ term is dominated by the LT contribution (Fig.9.d).

8. Conclusions

As remembered in Sec.1, the investigation of indirect signal of New Physics results of many strong theoretical motivations. The actual precision tests on Boson-Fermion interactions being in agreement with the standard predictions with a high level of accuracy, we have chosen to probe the existence of NP through the precise and direct test of the bosonic self interactions which should be feasible at the next generation of hadron colliders. Leaving the four boson couplings for a separate analysis, we restricted ourself to the test of the Three Gauge Boson couplings predicted by the Standard Model.

In this paper we have given several calculation tools which should be useful to probe the most general structure of the WWV ($V = \gamma$ or Z) vertex in a model independent way through the precise measurement of the W^+W^- , $W^\pm Z$ and $W^\pm\gamma$ bosonic pair production. In Sec.5 and 6, we have computed the helicity amplitudes for the production of all TGV-sensitive two boson final states via quark-antiquark annihilation. We deduced from these Tables the full analytic expressions of the tree level Cross-Sections for all productions and in function of the 14 free parameters of the most general WWV ($V = \gamma, Z$) effective Lagrangian. These Cross-Sections should be very useful to predict the sensitivity of present and future proton-(anti)proton colliders to the complete set of anomalous trilinear couplings given in Sec.2. We exhibit in Sec.8 the sensitivity of the invariant mass and the transverse momentum distributions studied in Sec.3 and 7 to the various anomalous couplings for $W^\pm Z$ and $W^\pm\gamma$ productions. Some other hadronic observables as the amplitude zeros, the rapidity correlations and cross section ratios should also be sensitive [23, 25, 31] and can be tested in performing a model-independent multi-parameter analysis of real or simulated data through fits and shapes of contour plots. In the eventuality where a significant departure from the standard expectations is measured, the exploration of the underlying NP through bosonic sector will be indissociable from an identification of the anomalous couplings responsible for this deviation. This goes unavoidably through the disentangling of the 14 free parameters effects of the full effective TGV Lagrangian (1).

As anomalous couplings contribute to helicity amplitudes given in Tables 2 to 4 with different weights, we show in Sec.7 that the identification of the Longitudinal or Transverse polarization of both final bosons will be very useful to separate those effects.

In conclusion, we find that if one identifies the polarization state of the final W and Z bosons and in the case where only one anomalous coupling is supposed to be non-zero at a time, the helicity Table 3 should allow us to identify and separate the contributions of all the seven WWZ anomalous couplings δ_Z , x_Z , y_Z , z_Z , z'_{1Z} , z'_{2Z} , z'_{3Z} , through the analysis of the $W^\pm Z$ production only.

On the contrary, given the helicity Table 4, only the existence of non-zero δ_γ , x_γ , $z'_{1\gamma}$ or $z'_{2\gamma}$ couplings can be tested through single $W^\pm\gamma$ production without possibility to identify from which coupling came the deviation. Nevertheless, the y_γ and z_γ couplings should be clearly separated from the others through an analysis of the final W^\pm polarization states in $W^\pm\gamma$ process only. A complete separation of the effects of the other $WW\gamma$ anomalous couplings needs an additional analysis.

These properties which allow a clear separation of the different types of WWV , ($V = Z$ or γ) couplings can only be achieved if one has enough luminosity for providing a large number of bosonic pair events decaying both in leptonic final state. Due to the high luminosity expected at LHC and the future luminosity upgrade at FERMILAB, this condition should be realized in the next 10 years at least.

Finally, we stress that the analytic expressions of the helicity Tables and Cross-Section given in this paper should be very suitable for a general model independent study of the sensitivity of actual and future measurements to an indirect signal of NP in the bosonic sector [§].

9. Acknowledgments

I would like to thank J.L. Kneur for his very helpful suggestions in writing the Fortran codes. I am especially grateful to J. Layssac, F.M. Renard and G. Moutaka for many valuable and stimulating discussions and a critical reading of the manuscript.

[§] All relevant analytic expressions are available upon request by E.Mail at: NUSS@lpm.univ-montp2.fr

9. References

1. See e.g. the talk given by S.Dawson at the *DPF 96* annual meeting, hep-ph/9609340 and J.L.Hewett, T.Takeuchi and S.Thomas, SLAC-PUB-7088. See also The LEP Electroweak Working Group, *Internal note* LEPEWWG/95-02 (CERN, 1 Aug.1995) and The LEP Electroweak Heavy Flavours Working Group, *Internal note* LEPHF/95-02 (CERN, 25 Jul. 1995); SLC Collaboration, as presented at C.E.R.N. by C.Baltay (June 1995).
2. See e.g. Dong Su, SLD Collaboration, Talk given at Warshaw conference on High Energy Physics (1996) and L.Piemontese, Talk given at the Workshop "Lepton Polarization at High Energy Colliders", Lecce, Italy, Sept.1996.
3. CDF Collaboration, D.Neuberger, CDF-PUB-ELECTROWEAK-PUBLIC-3371; CDF Collaboration, F.Abe et al., *Phys. Rev. Lett.* **74** (1995) 1936 and *Phys. Rev. Lett.* **75** (1995) 1017 ; D0 Collaboration, S.Abachi et al., *Phys. Rev. Lett.* **75** (1995) 1023 and *Phys. Rev. Lett.* **75** (1995) 1034 ; CDF Collaboration, A.Barnett, FERMILAB-CONF-96-039-E.
4. W.Lee, C.Quigg and H.B. Thacker, *Phys. Rev.* **D16** (1977) 1519 ; S.Chanowitz, *Eloisatron Workshop: Higgs* 1989:311-332 (QCD161:I12:1989); S.Chanowitz, *Perspectives on Higgs Physics: 343-395* (QCD161:K365).
5. S.L.Glashow, *Nucl. Phys.* **22** (1961) 579 ; S.Weinberg, *Phys. Rev. Lett.* **19** (1967) 1264 ; A.Salam, in *Proceedings of the Eighth Nobel Symposium*, edited by N.Svartholm (Almqvist and Wiksell, Stockholm, Wiley, New York, 1968), p.367.
6. T.G.Rizzo, *Phys. Rev.* **D32** (1985) 43 ; T.Appelquist and Guo-Hong Wu, *Phys. Rev.* **D48** (1993) 3235 ; T.L.Barklow, S.Dawson, H.E.Haber and J.L.Siegrist, SLAC-PUB-95-6893, hep-ph/9505296.
7. G.Bélanger and F.Boudjema, *Phys. Lett.* **B288** (1992) 201 and *Phys. Lett.* **B288** (1992) 210 ; G.Abu Leil and W.J.Stirling, DTP-94-10 (preprint, June 1994); hep-ph/9406317; O.J.P.Éboli, M.C.González-Garcia and S.F.Novaes, *Nucl. Phys.* **B411** (1994) 381 ; F.Cuyppers and K.Kolodziej, *Phys. Lett.* **B344** (1995) 365 .
8. K.Hagiwara, S.Ishihara, R.Szalapski and D.Zeppenfeld, *Phys. Lett.* **B283** (1992) 353 and *Phys. Rev.* **D48** (1993) 2182 ; A.De Rújula, M.B. Gavela, P. Hernandez and E. Massó, *Nucl. Phys.* **B384** (1992) 3 .
9. S.Weinberg, *Physica* **96A** (1979) 327; J. Polchinski, *Nucl. Phys.* **B231** (1984) 269 ; H.Georgi, *Weak Interactions and Modern Particle Theory* (Benjamin/Cummings Menlo Park, 1984); C.P.Burgess and J.A.Robinson, in *BNL Summer Study on CP Violation*; S.Dawson and A.Soni editors, (World Scientific, Singapore, 1991).
10. F.M.Renard, *Nucl. Phys.* **B196** (1982) 93 ; A.Barroso, F.Boudjema, J.Cole, and N.Dombey, *Z. Phys.* **C28** (1985) 149 ; U.Baur and E.L.Berger, *Phys. Rev.* **D47** (1993) 4889 ; D.Choudhury and S.D.Rindani, *Phys. Lett.* **B335** (1994) 198 .
11. K.J.F.Gaemers and G.J.Gounaris, *Z. Phys.* **1** (1979) 259 ; K.Hagiwara, R.Peccei, D.Zeppenfeld and K.Hikasa, *Nucl. Phys.* **B282** (1987) 253 .

12. G.J.Gounaris, J.Layssac, G.Moultaka and F.M.Renard, *INT. J. MOD. PHYS. A*, vol.8,No.19(1993) 3285; M.Bilenky, J.-L.Kneur, F.M.Renard and D.Schildknecht, npB409199322.
13. W.A.Bardeen, R.Gastmans and B.Lautrup, *Nucl. Phys.* **B46** (1972) 319 ; G.Couture and J.N.Ng, *Z. Phys.* **C35** (1987) 65 ; E.N.Argyres, G.Katsilieris, A.B.Lahanas, C.G.Papadopoulos and V.C.Spanos, *Nucl. Phys.* **B391** (1993) 23 ; J.Papavassiliou and K.Philippides, *Phys. Rev.* **D48** (1993) 4255 ; J.Fleischer, J.-L.Kneur, K.Kolodziej, M.Kuroda and D.Schildknecht, *Nucl. Phys.* **B378** (1992) 443 , (E): *ibid.* **B426**(1994) 246.
14. A.B.Lahanas and V.C.Spanos, *Phys. Lett.* **B334** (1994) 378 ; A.Arhib, J.-L.Kneur and G.Moultaka, hep-ph/9512437, to appear in *Phys. Lett. B*; E.N.Argyres, A.B.Lahanas, C.G.Papadopoulos and V.C.Spanos, Preprint UA/NPPS-18B (October 95).
15. G.J.Gounaris, F.M.Renard and G.Tsirigoti, *Phys. Lett.* **B338** (1994) 51 ; G.J.Gounaris, F.M.Renard and G.Tsirigoti, *Phys. Lett.* **B350** (1995) 212 ; J.Wudka, in *Physics and Technology of the Next Linear Collider*, eds. D.Burke and M.Peskin, hep-ph/9606478.
16. G.J.Gounaris and F.M.Renard, *Z. Phys.* **C59** (1993) 133 .
17. M.Kuroda, F.M.Renard and D. Schildknecht, *Phys. Lett.* **B183** (1987) 366 ; M.B.Einhorn and J.Wudka, preprints NSF-ITP-92-01 (1992) and UM-TH-92-25 (1992); C.P.Burgess and D.London, *Phys. Rev. Lett.* **69** (1992) 3428 , and *Phys. Rev.* **D48** (1993) 4337 ; J.Wudka, *Int. J. Mod. Phys.* **A9** (1994) 2301; C.Grosse-Knetter, I.Kuss and D.Schildknecht, *Phys. Lett.* **B358** (1995) 87 ; C.Arzt, M.B.Einhorn, and J.Wudka, *Phys. Rev.* **D49** (1994) 1370 and *Nucl. Phys.* **B433** (1995) 41 .
18. C.J.C.Burges and H.J.Schnitzer, *Nucl. Phys.* **B228** (1983) 464 ; W.Buchmüller and D.Wyler, *Nucl. Phys.* **B268** (1986) 621 ; C.N.Leung, S.T.Love and S.Rao, *Z. Phys.* **C31** (1986) 433 .
19. E.N.Argyres and C.G.Papadopoulos, *Phys. Lett.* **B263** (1991) 298 ; D.Zeppenfeld, Waikoloa Linear Collid.1993: 695-703 (QCD183:I795:1993), hep-ph/9307333; C.G.Papadopoulos, *Phys. Lett.* **B333** (1994) 202 ; S.Dawson and G.Valencia, Warsaw 1994, Proceedings, *Physics from Planck scale to electroweak scale* 104-115, hep-ph/9411262; K.Hagiwara, S.Matsumoto and R.Szalapski, *Phys. Lett.* **B357** (1995) 411 ; Report of the ‘Triple Gauge Boson Couplings’ Working Group, G.J.Gounaris, J-L.Kneur and D.Zeppenfeld (convenors), in *Physics at LEP2*, eds. G.Altarelli, T.Sjöstrand and F.Zwirner, CERN Report 96-01 (1996).
20. G.J.Gounaris, J.Layssac and F.M.Renard, *Phys. Lett.* **B332** (1994) 146 ; G.J.Gounaris, J.Layssac, J.E.Paschalis and F.M.Renard, *Z. Phys.* **C66** (1995) 619
21. U.Baur and D.Zeppenfeld, *Phys. Lett.* **B201** (1988) 383 ; U.Baur and D.Zeppenfeld, *Nucl. Phys.* **B308** (1988) 127 .
22. The LHC Study Group, ”Design Study of the Large Hadron Collider”, Report No.

- CERN 91-03, 1991 (unpublished).
23. U.Baur, T.Han and J.Ohnemus, *Phys. Rev.* **D51** (1995) 3381 .
 24. R.W.Brown, D.Sahdev and K.O.Mikaelian, *Phys. Rev.* **D20** (1979) 1164 ;
R.W.Brown and K.O.Mikaelian, *Phys. Rev.* **D19** (1979) 922 ; D.Zeppenfeld and
S.Willenbrock, *Phys. Rev.* **D37** (1988) 1775 ; G.L.Kane, J.Vidal and C.P.Yuan,
Phys. Rev. **D39** (1989) 2617 ; G.Martinelli et al., *ECFA Workshop on LHC
Physics*, Aachen 1990; D.Zeppenfeld, *International Symposium on Vector Boson
Self-interactions*, hep-ph/9506239;
F.M.Renard, *Festkolloquium* D.Schildknecht, Bielefeld, hep-ph/9501305.
 25. K.O.Mikaelian, A.Samuel and D.Sahdev, *Phys. Rev. Lett.* **43** (1979) 746 ; U.Baur
and E.L.Berger, *Phys. Rev.* **D41** (1990) 1476 ; U.Baur, T.Han and J.Ohnemus,
Phys. Rev. Lett. **72** (1994) 3941 ; Aihara et al., Summary of the Working Subgroup
on Anomalous Gauge Boson Interactions of the DPF Long Range Planning Study,
report FERMILAB-Pub-95/031 (1995), hep-ph/9503425.
 26. J.M.Cornwall, D.N.Levin, and G.Tiktopoulos, *Phys. Rev. Lett.* **30** (1973) 1268
and *Phys. Rev.* **D10** (1974) 1145 ; C.H.Llewellyn Smith, *Phys. Lett.* **B46** (1973)
233 ; S.D.Joglekar, *Ann. Phys.* **83**, 427 (1974).
 27. R.P.Feynman, "Photon-Hadron Interactions", ed. *Frontiers in Physics* (1972).
 28. V.Barger, K.Cheung, T.Han and R.J.N.Phillips, *Phys. Rev.* **D42** (1990) 3052
; J.Bagger, V.Barger, K.Cheung, J.Gunion, T.Han, G.A.Ladinsky, R.Rosenfeld,
and C.-P.Yuan, *Phys. Rev.* **D49** (1994) 1246 and *Phys. Rev.* **D52** (1995) 3878 ;
I.Kuss and H.Spiesberger, *Phys. Rev.* **D53** (1996) 6078 ; S.N.Gupta, J.M.Johnson,
G.A.Ladinsky and W.W. Repko, *Phys. Rev.* **D53** (1996) 4897 .
 29. E.Eichten, I.Hinchliffe, K.Lane and C.Quigg, *Rev.Mod.Phys.* 56(1984)579.
 30. A.D.Martin, R.G.Roberts and W.J.Stirling, *Rutherford preprint* RAL-95-021
(1995), hep-ph/9502336.
 31. G.J.Gounaris and F.M.Renard, *Z. Phys.* **C59** (1993) 143 .
 32. P.Mery, M.Perrottet and F.M.Renard, *Z. Phys.* **C36** (1987) 249 .
 33. F.M.Renard: "Basics of e^+e^- collisions", ed. *Frontières* (1981).
 34. G.J Gounaris, J.Layssac and F.M.Renard, *Z. Phys.* **C62** (1994) 139 .
 35. R.L.Sekulin, *Phys. Lett.* **B338** (1994) 369 . See also, for example, R.Barlow,
Statistics (John Wiley and Sons, Chichester, 1989) p. 90 or *Statistical methods in
experimental physics*, W.T.Eadie et al., North Holland Publishing, 1971.
 36. D.Atwood and A.Soni, *Phys. Rev.* **D45** (1992) 2405 ; M.Davier, L.Duflot, F.Le
Diberder, A.Rougé, *Phys. Lett.* **B306** (1993) 411 ; ALEPH Collaboration, *Z.
Phys.* **C59** (1993) 369 ; P.Overmann, preprint DO-TH 93/24, Dortmund, 1993 ;
M.Diehl and O.Nachtmann, *Z. Phys.* **C62** (1994) 397 .

List of Tables

- Table 1: Decomposition of the helicity basis.
 Table 2: Helicity Table for W^+W^- production.
 Table 3: Helicity Table for $W^\pm Z$ production. $\eta = \mp 1$ for W^\pm production.
 Table 4: Helicity Table for $W^\pm\gamma$ production. $\eta = \mp 1$ for W^\pm production.
 Table 5: Helicity Tables for $ZZ, Z\gamma$ and $\gamma\gamma$ production.
 Table 6: $\mathcal{F}_{WW}^{\xi, \xi'}(i)$ coefficients for W^+W^- production.
 Table 7: Standard $\mathcal{O}_{WW}^{\xi, \xi'}(i)$ coefficients for W^+W^- production.
 Table 8: Non standard $\mathcal{O}_{WW}^{\xi, \xi'}(i)$ coefficients for W^+W^- production.
 Table 9: $\mathcal{F}_{WV}^{\xi, \xi'}(i)$ coefficients for $W^\pm Z$ and $W^\pm\gamma$ production.
 Table 10: Standard $\mathcal{O}_{WZ}^{\xi, \xi'}(i)$ coefficients for $W^\pm Z$ production.
 Table 11: Non standard $\mathcal{O}_{WZ}^{\xi, \xi'}(i)$ coefficients for $W^\pm Z$ production.
 Table 12: Standard $\mathcal{O}_{W\gamma}^{\xi, \xi'}(i)$ coefficients for $W^\pm\gamma$ production.
 Table 13: Non standard $\mathcal{O}_{W\gamma}^{\xi, \xi'}(i)$ coefficients for $W^\pm\gamma$ production.
 Table 14: Standard $\mathcal{O}_{VV'}^{\xi, \xi'}(i)$ and $\mathcal{F}_{VV'}^{\xi, \xi'}(i)$ coefficients for $\mathbf{q}_i^{(\prime)} \bar{\mathbf{q}}_i^{(\prime)} \rightarrow \mathbf{V}\mathbf{V}'$ with $VV' = ZZ, Z\gamma, \gamma\gamma$.

List of Figures

- Fig.1 Bosonic pair production via Bosons fusion (a) and quarks annihilation (b).
 Fig.2 Feynman graphs for W^+W^- production.
 Fig.3 W^+W^-V vertex.
 Fig.4 Feynman graphs for $W^\pm Z$ and $W^\pm\gamma$ productions.
 Fig.5 $W^\pm W^\pm V$ vertex.
 Fig.6 Invariant Mass distributions for $W^\pm Z$ (Fig.6.a) and $W^\pm\gamma$ (Fig.6.b) productions with various non-zero anomalous couplings.
 Fig.7 Transverse Momentum distributions for $W^\pm Z$ (Fig.7.a) and $W^\pm\gamma$ (Fig.7.b) productions with various non-zero anomalous couplings.
 Fig.8 Longitudinal(L) and Transverse(T) final state polarizations in Standard Momentum distribution (Fig.8.a) and with anomalous couplings for $W^\pm Z$ production: δ_Z (Fig.8.b), x_Z (Fig.8.c), y_Z (Fig.8.d), z_Z (Fig.8.e) and z'_{1Z} (Fig.8.f), z'_{2Z} (Fig.8.g) and z'_{3Z} (Fig.8.h).
 Fig.9 Longitudinal(L) and Transverse(T) final state polarizations for $W^\pm\gamma$ production in Standard Momentum distribution (Fig.9.a) and with anomalous couplings: x_γ (Fig.9.b), y_γ (Fig.9.c) and z_γ (Fig.9.d).

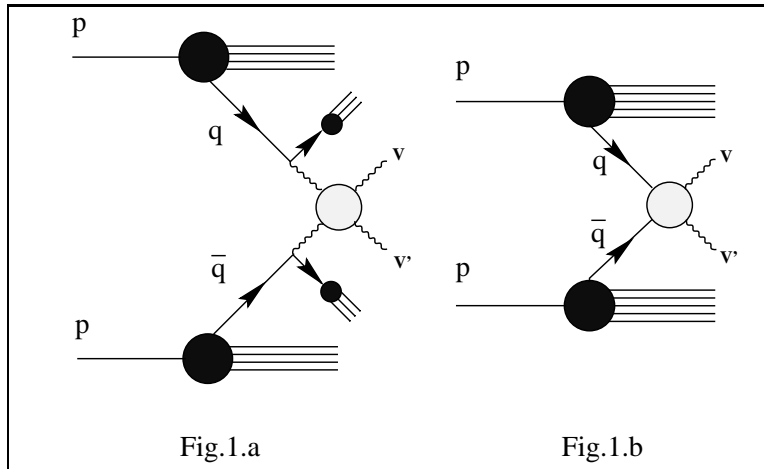


Figure 1: Bosonic pair production via Bosons fusion (a) and quarks annihilation (b).

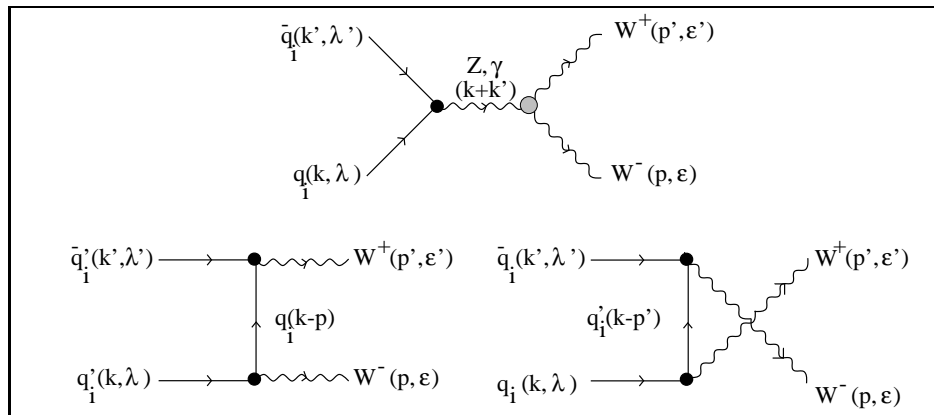
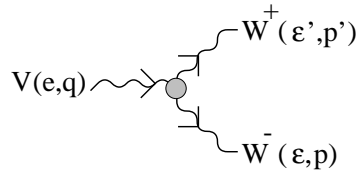


Figure 2: Feynman graphs for W^+W^- production.



$$i\mathcal{L} = -iee_V^\mu \mathcal{V}_\mu^V$$

Figure 3: W^+W^-V vertex.

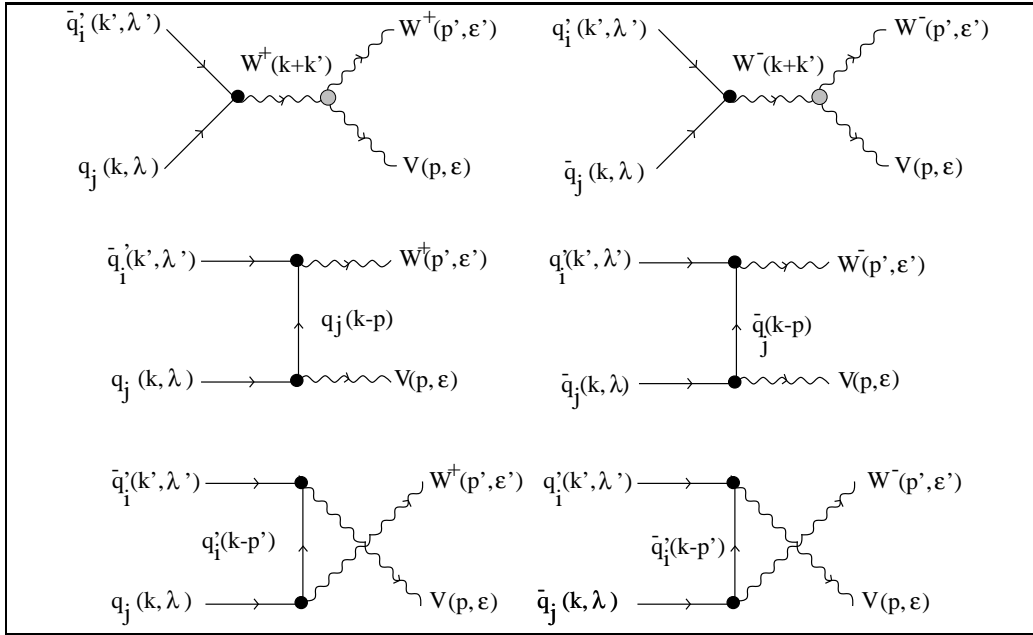
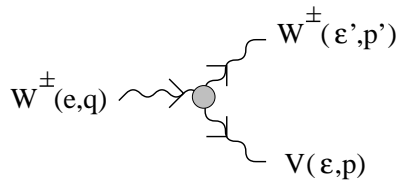


Figure 4: Feynman graphs for $W^\pm Z$ and $W^\pm \gamma$ productions.



$$i\mathcal{L} = -iee_W^\mu \mathcal{V}_\mu^V$$

Figure 5: $W^\pm W^\pm V$ vertex.

$$pp \rightarrow W^+ Z \rightarrow l_1^+ \nu_1 l_2^+ l_2^- + X$$

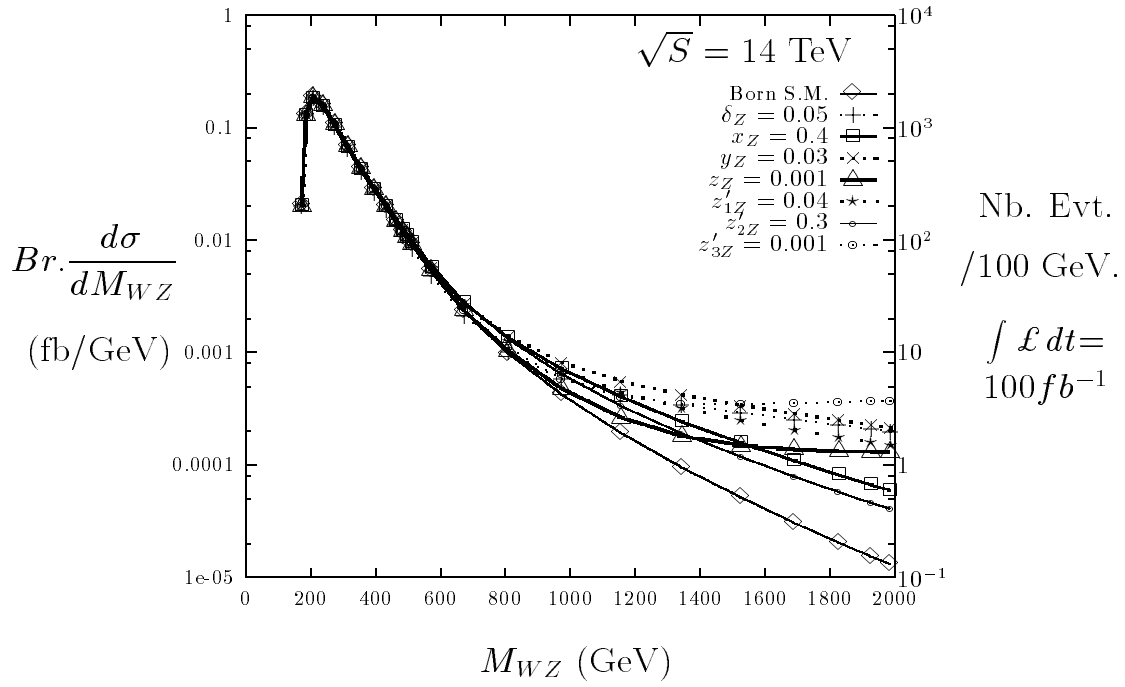


Figure 6.a

$$pp \rightarrow W^+ \gamma \rightarrow l^+ \nu \gamma + X$$

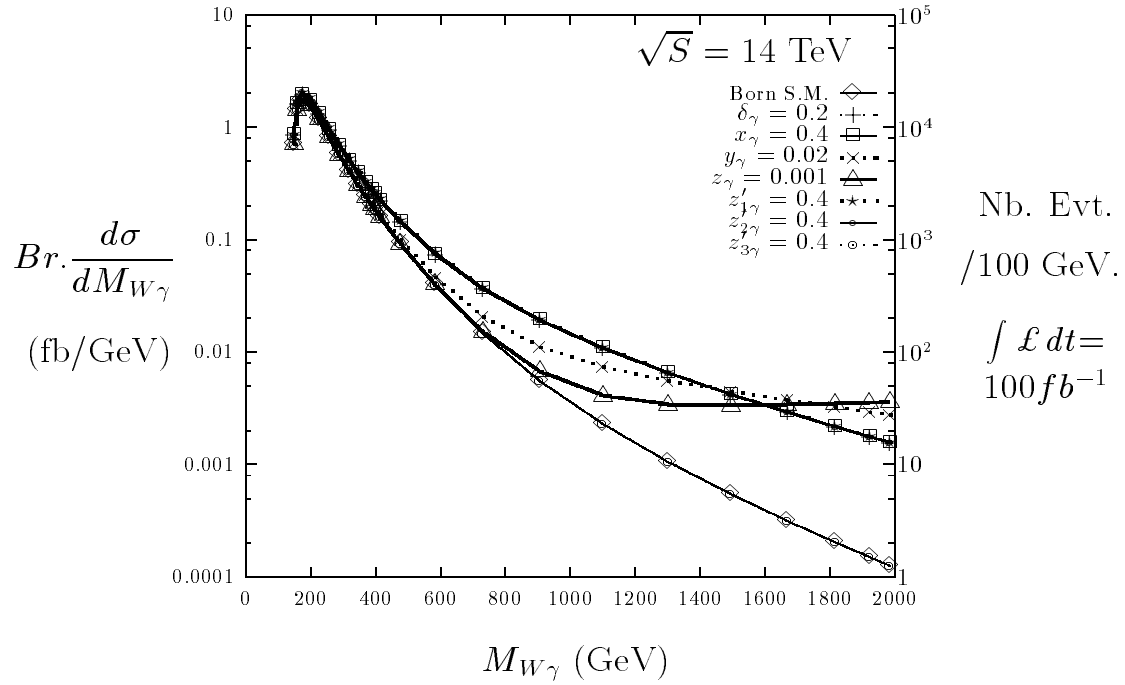


Figure 6.b

Invariant Mass distributions for $W^\pm Z$ (Fig.6.a) and $W^\pm \gamma$ (Fig.6.b) productions with various non-zero anomalous couplings.

$$pp \rightarrow W^+ Z \rightarrow l_1^+ \nu_1 l_2^+ l_2^- + X$$

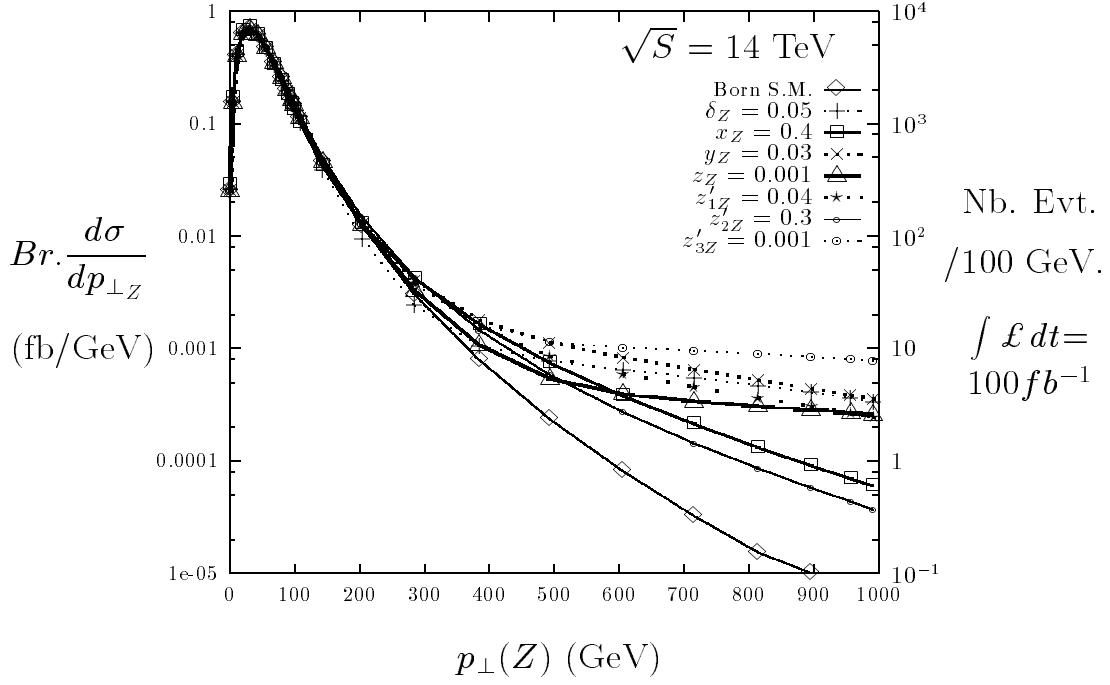


Figure 7.a

$$pp \rightarrow W^+ \gamma \rightarrow l^+ \nu \gamma + X$$

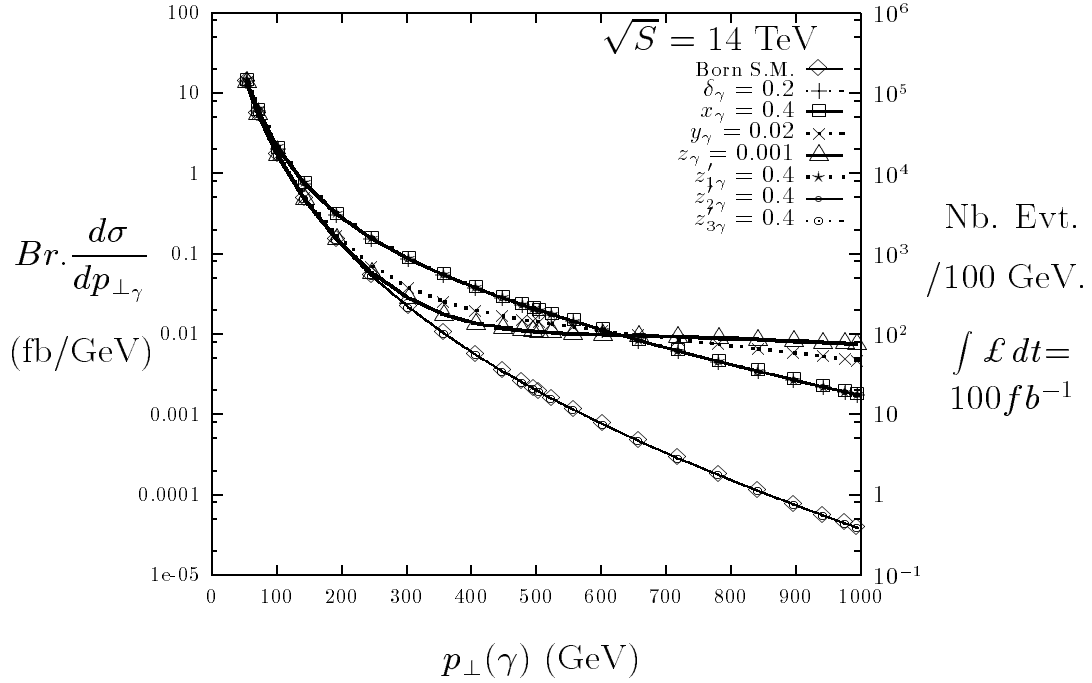


Figure 7.b

Transverse Momentum distributions for $W^\pm Z$ (Fig.7.a) and $W^\pm \gamma$ (Fig.7.b) productions with various non-zero anomalous couplings.

$$pp \rightarrow W^+ Z \rightarrow l_1^+ \nu_1 l_2^+ l_2^- + X$$

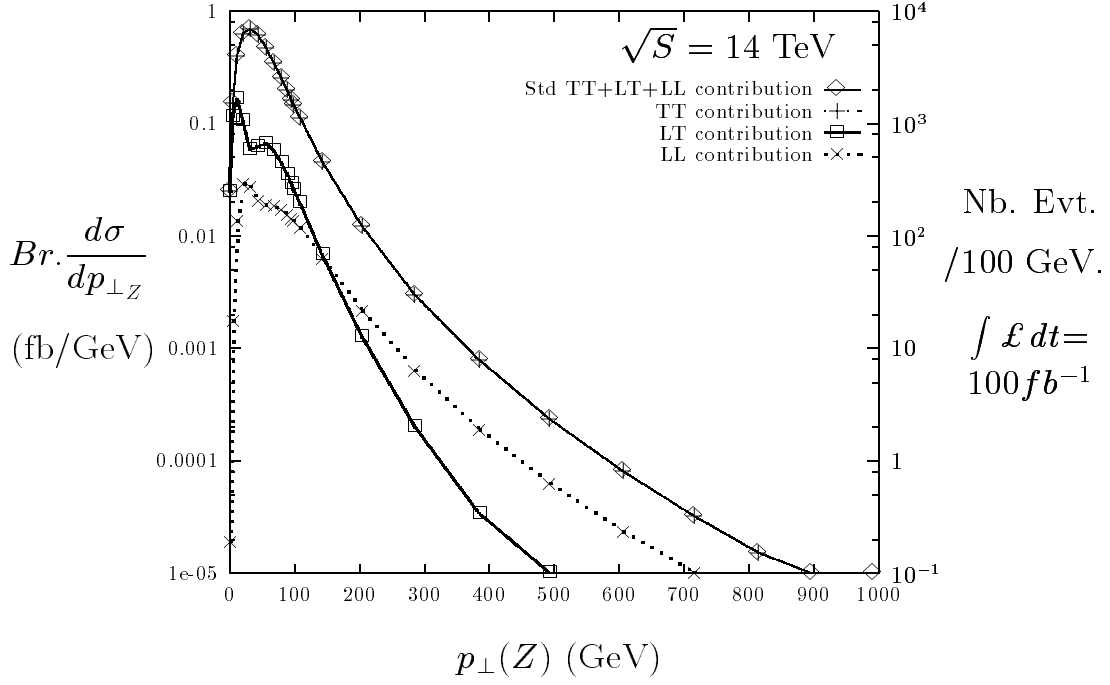


Figure 8.a

$$pp \rightarrow W^+ Z \rightarrow l_1^+ \nu_1 l_2^+ l_2^- + X$$

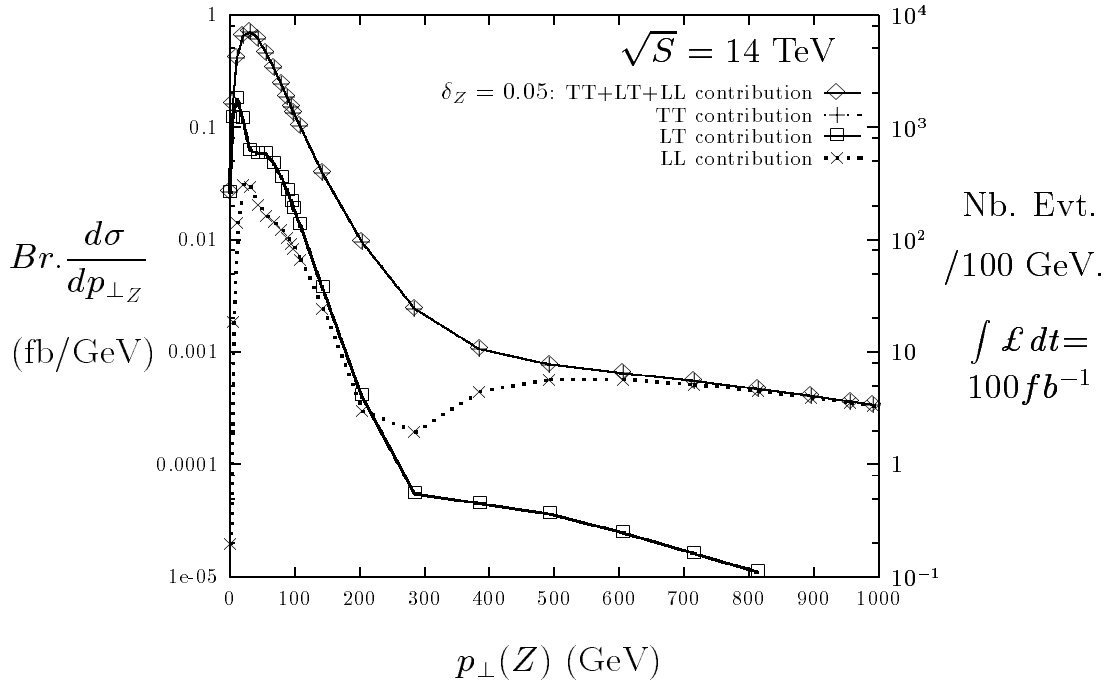


Figure 8.b

Longitudinal(L) and Transverse(T) final state polarizations in Standard Momentum distribution (Fig.8.a) and with anomalous δ_Z coupling (Fig.8.b) for $W^\pm Z$ production.

$$pp \rightarrow W^+ Z \rightarrow l_1^+ \nu_1 l_2^+ l_2^- + X$$

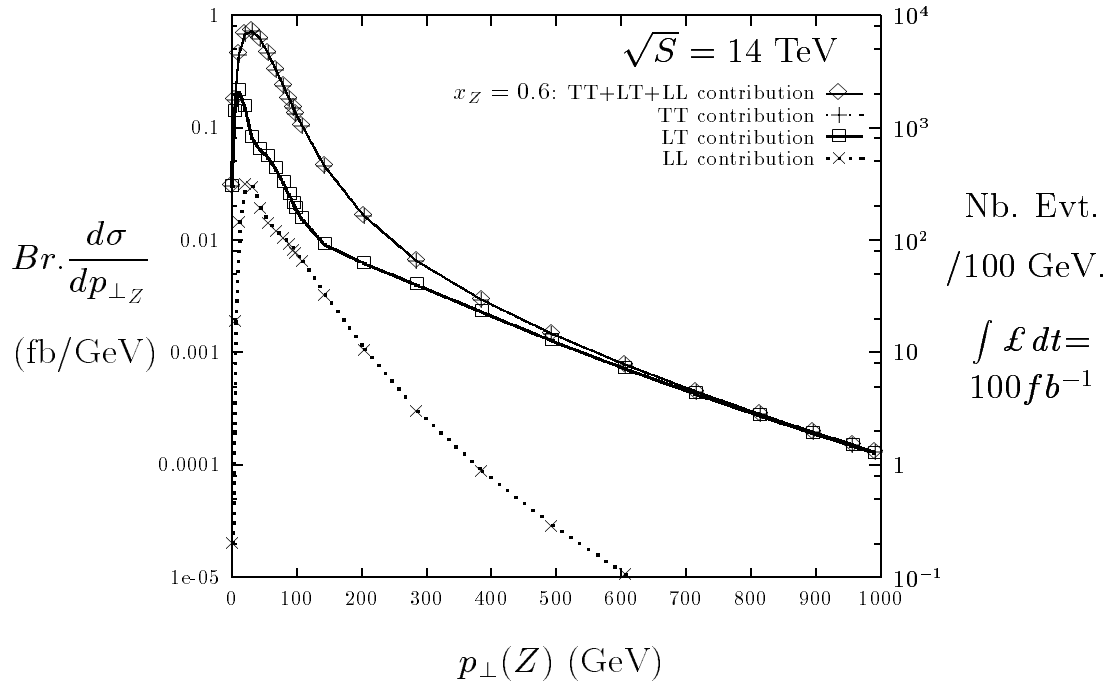


Figure 8.c

$$pp \rightarrow W^+ Z \rightarrow l_1^+ \nu_1 l_2^+ l_2^- + X$$

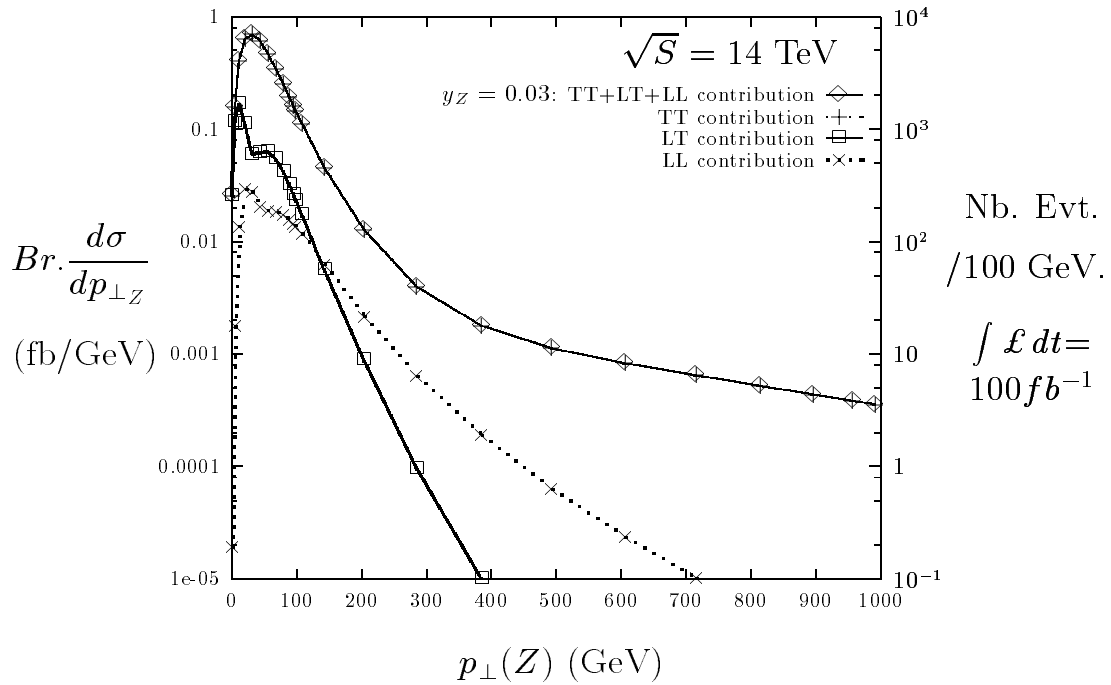


Figure 8.d

Longitudinal(L) and Transverse(T) final state polarizations in Momentum distribution for $W^{\pm}Z$ production with anomalous x_Z (Fig.8.c) and y_Z (Fig.8.d) couplings.

$$pp \rightarrow W^+ Z \rightarrow l_1^+ \nu_1 l_2^+ l_2^- + X$$

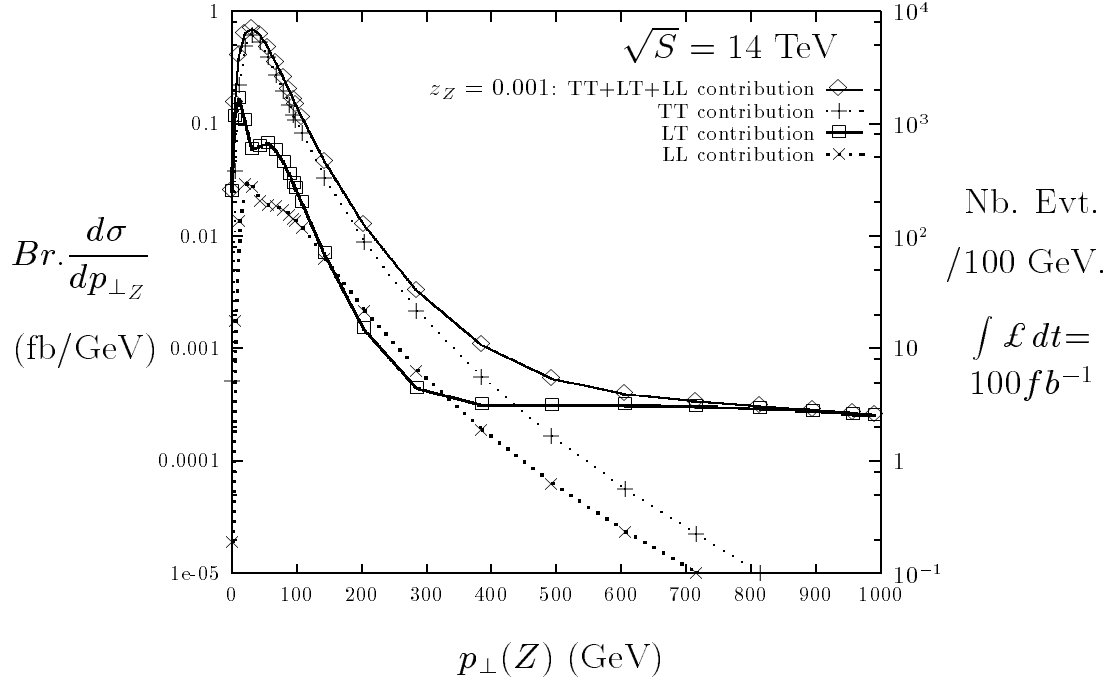


Figure 8.e

$$pp \rightarrow W^+ Z \rightarrow l_1^+ \nu_1 l_2^+ l_2^- + X$$

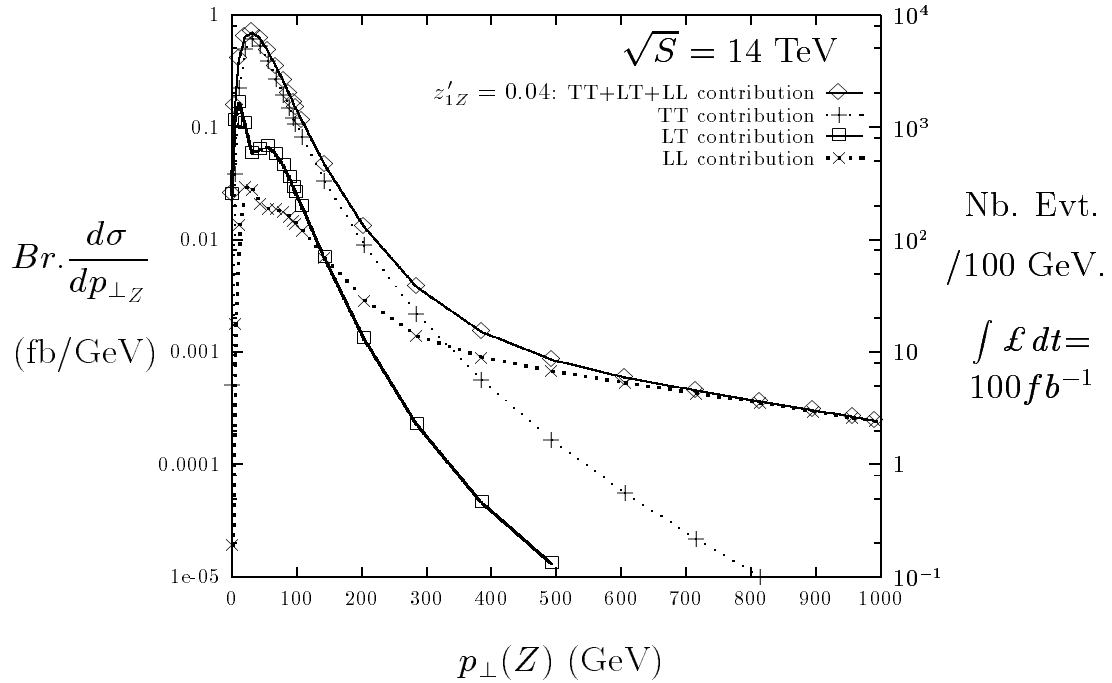


Figure 8.f

Longitudinal(L) and Transverse(T) final state polarizations in Momentum distribution for $W^\pm Z$ production with anomalous z_Z (Fig.8.e) and z'_{1Z} (Fig.8.f) couplings.

$$pp \rightarrow W^+ Z \rightarrow l_1^+ \nu_1 l_2^+ l_2^- + X$$

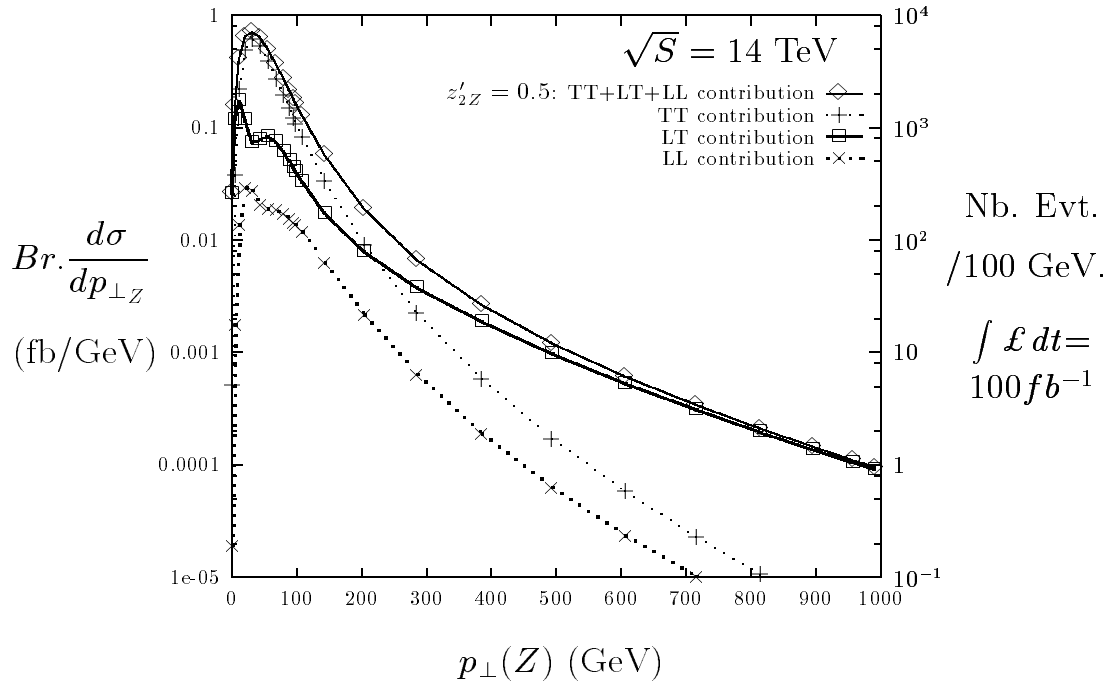


Figure 8.g

$$pp \rightarrow W^+ Z \rightarrow l_1^+ \nu_1 l_2^+ l_2^- + X$$

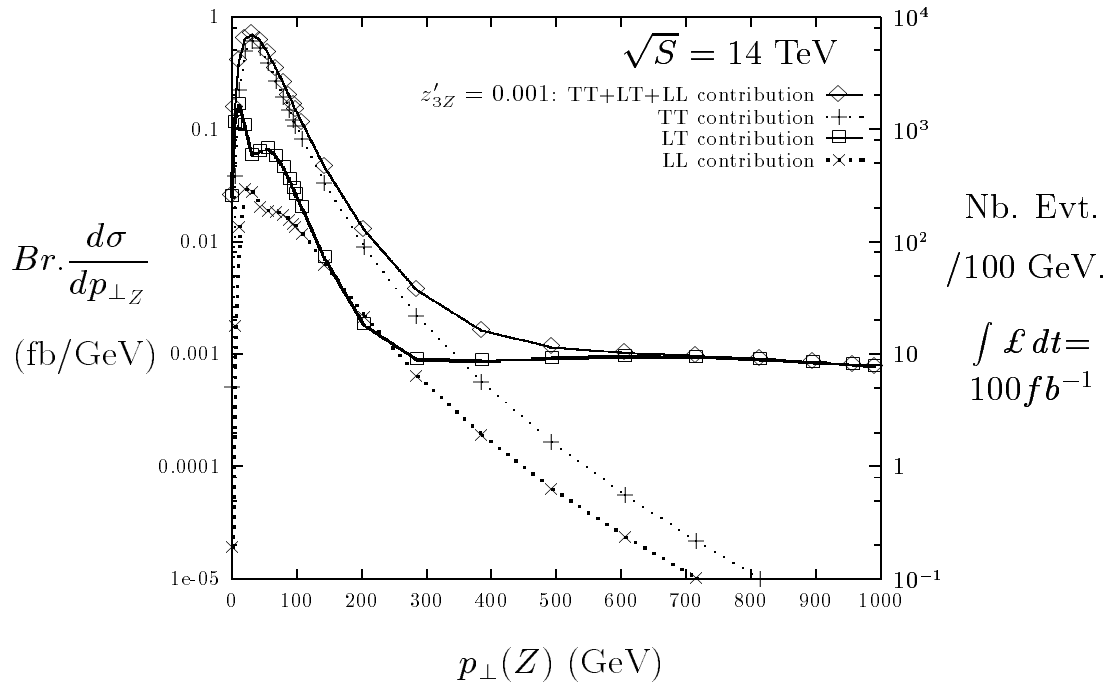


Figure 8.h

Longitudinal(L) and Transverse(T) final state polarizations in Momentum distribution for $W^\pm Z$ production with anomalous z'_{2Z} (Fig.8.g) and z'_{3Z} (Fig.8.h) couplings.

$$pp \rightarrow W^+ \gamma \rightarrow l^+ \nu \gamma + X$$

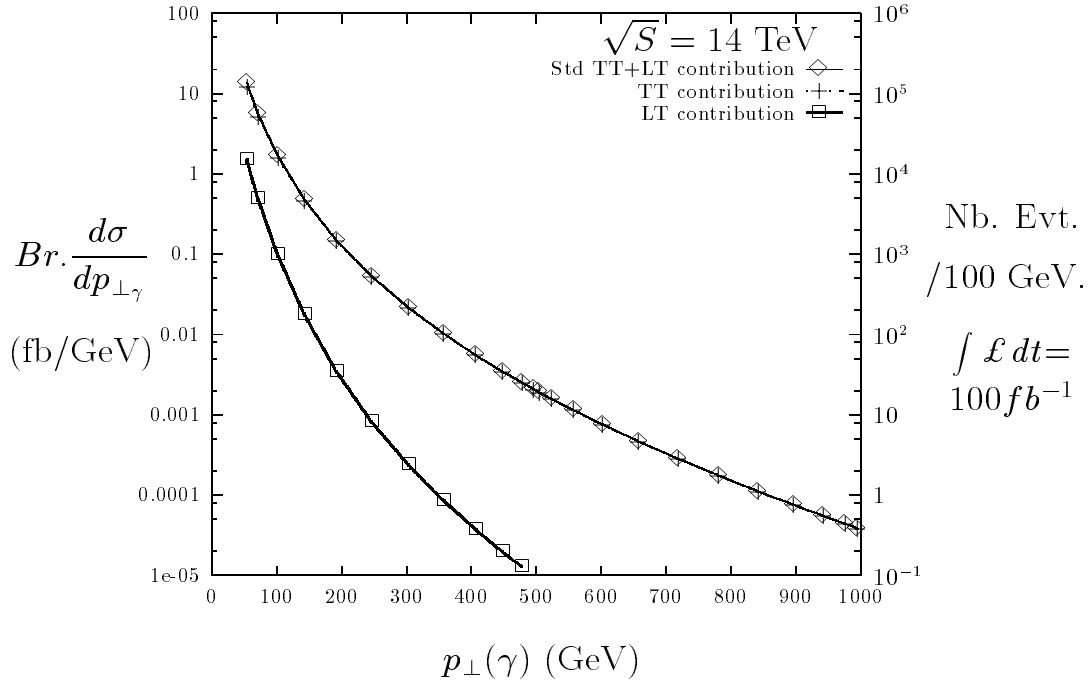


Figure 9.a

$$pp \rightarrow W^+ \gamma \rightarrow l^+ \nu \gamma + X$$

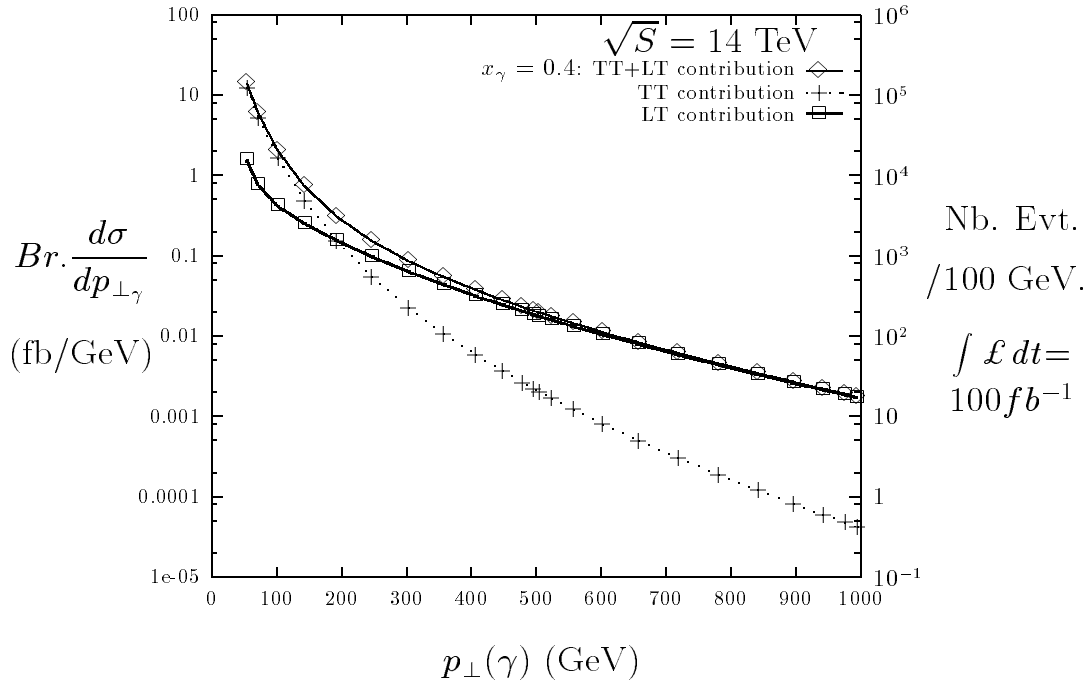


Figure 9.b

Longitudinal(L) and Transverse(T) final state polarizations in Standard Momentum distribution (Fig.9.a) and with anomalous x_{γ} coupling (Fig.9.b) for $W^{\pm} \gamma$ production. The δ_{γ} , $z'_{1\gamma}$ and $z'_{2\gamma}$ couplings have the same contribution as x_{γ} .

$$pp \rightarrow W^+ \gamma \rightarrow l^+ \nu \gamma + X$$

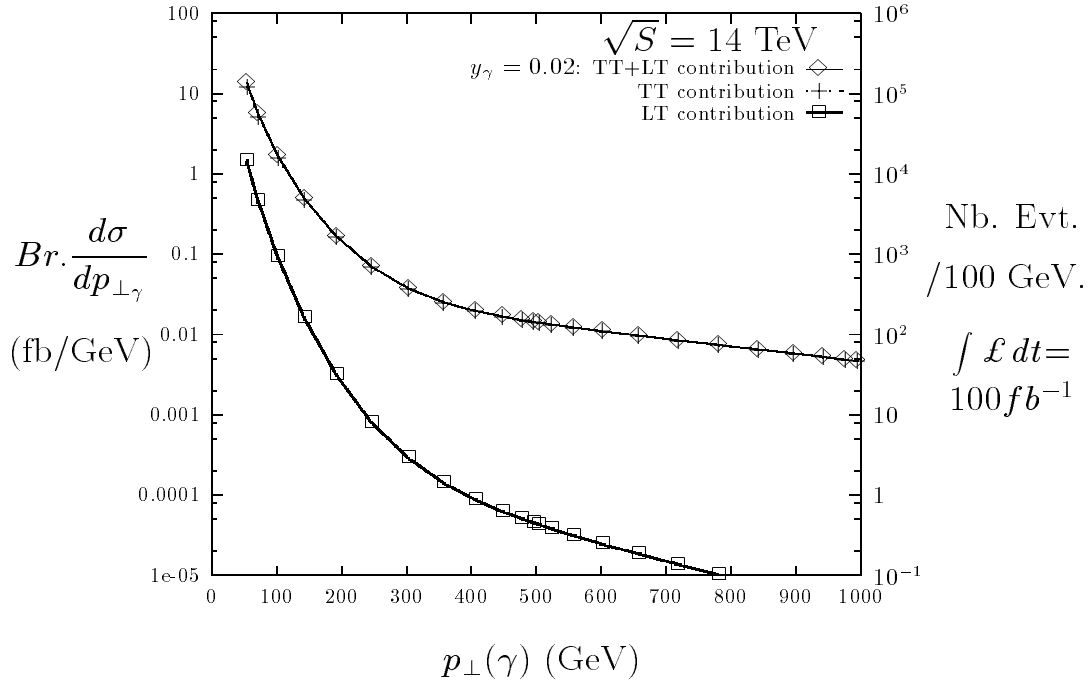


Figure 9.c

$$pp \rightarrow W^+ \gamma \rightarrow l^+ \nu \gamma + X$$

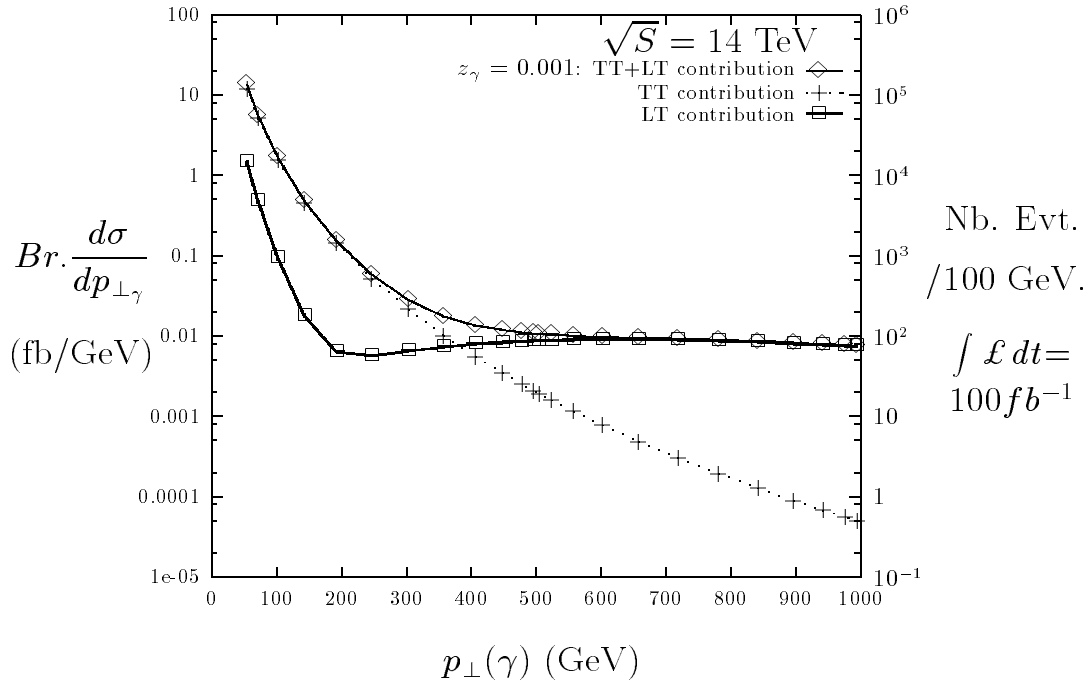


Figure 9.d

Longitudinal(L) and Transverse(T) final state polarizations in Momentum distribution for $W^\pm \gamma$ production with anomalous y_γ (Fig.9.c) and z_γ couplings (Fig.9.d).

Table 1: Decomposition of the helicity basis.

| | $\tau = \tau' = \pm 1$ | $\tau = -\tau' = \pm 1$ | $\tau = \tau' = 0$ | $\tau = 0, \tau' = \pm 1$ | $\tau = \pm 1, \tau' = 0$ |
|-----------------|--|---|---|--|---|
| \mathcal{N}_1 | $-\frac{1}{2}\tau \sin \theta (\tau \cos \theta - 2\lambda)$ | $\frac{1}{2}\tau \sin \theta (\tau \cos \theta + 2\lambda)$ | $-\frac{e'}{mm'} \sin \theta (\vec{p} + e \cos \theta)$ | $-\frac{1}{\sqrt{2m}} (\tau' \cos \theta - 2\lambda) (\vec{p} + e \cos \theta)$ | $-\frac{e'}{\sqrt{2m'}} \tau \sin^2 \theta$ |
| \mathcal{N}_2 | $-\mathcal{N}_1$ | $-\mathcal{N}_1$ | $-\frac{e'}{mm'} \sin \theta (\vec{p} - e \cos \theta)$ | $-\frac{1}{\sqrt{2m}} (\tau' \cos \theta - 2\lambda) (\vec{p} - e \cos \theta)$ | $-\mathcal{N}_1$ |
| \mathcal{N}_3 | $-\frac{1}{2}\tau \sin \theta (\tau \cos \theta + 2\lambda)$ | \mathcal{N}_1 | $\frac{e}{mm'} \sin \theta (\vec{p} - e' \cos \theta)$ | $\frac{e}{\sqrt{2m}} \tau' \sin^2 \theta$ | $-\frac{1}{\sqrt{2m'}} (\tau \cos \theta + 2\lambda) (\vec{p} - e' \cos \theta)$ |
| \mathcal{N}_4 | $-\mathcal{N}_3$ | $-\mathcal{N}_1$ | $\frac{e}{mm'} \sin \theta (\vec{p} + e' \cos \theta)$ | $-\mathcal{N}_3$ | $-\frac{1}{\sqrt{2m'}} (\tau \cos \theta + 2\lambda) (\vec{p} + e' \cos \theta)$ |
| \mathcal{N}_5 | $-\beta \sin \theta$ | 0 | $\frac{1}{mm'} \beta \sin \theta (\vec{p} ^2 + ee')$ | 0 | 0 |
| \mathcal{N}_6 | $\frac{s}{8} \beta \sin^3 \theta$ | $-\frac{s}{8} \beta \sin^3 \theta$ | $-\frac{\sqrt{s} \sin \theta}{2mm'} \vec{p} (\vec{p} - e' \cos \theta) (\vec{p} - e \cos \theta)$ | $-\frac{\sqrt{s}}{2\sqrt{2m}} \tau' \sin^2 \theta \vec{p} (\vec{p} - e \cos \theta)$ | $+\frac{\sqrt{s}}{2\sqrt{2m'}} \tau \sin^2 \theta \vec{p} (\vec{p} - e' \cos \theta)$ |
| \mathcal{N}_7 | \mathcal{N}_6 | \mathcal{N}_6 | $-\frac{\sqrt{s} \sin \theta}{2mm'} \vec{p} (\vec{p} + e' \cos \theta) (\vec{p} + e \cos \theta)$ | $\frac{\sqrt{s}}{2\sqrt{2m}} \tau' \sin^2 \theta \vec{p} (\vec{p} + e \cos \theta)$ | $-\frac{\sqrt{s}}{2\sqrt{2m'}} \tau \sin^2 \theta \vec{p} (\vec{p} + e' \cos \theta)$ |
| \mathcal{N}_8 | $-\mathcal{N}_6$ | $-\mathcal{N}_6$ | $-\frac{\sqrt{s} \sin \theta}{2mm'} \vec{p} (\vec{p} + e' \cos \theta) (\vec{p} - e \cos \theta)$ | $-\mathcal{N}_6$ | $-\mathcal{N}_7$ |
| \mathcal{N}_9 | $-\mathcal{N}_6$ | $-\mathcal{N}_6$ | $-\frac{\sqrt{s} \sin \theta}{2mm'} \vec{p} (\vec{p} - e' \cos \theta) (\vec{p} + e \cos \theta)$ | $-\mathcal{N}_7$ | $-\mathcal{N}_6$ |

Table 2: Helicity Table for W^+W^- production.

| | | $\tau = \tau' = \pm 1$ | $\tau = -\tau' = \pm 1$ | $\tau = \tau' = 0$ | $\tau = 0, \tau' = \pm 1$ | $\tau = \pm 1, \tau' = 0$ |
|--------|---|--|--|---|--|---|
| | 1 | $\frac{-e^2 s \lambda}{2} \sin \theta$ | $\frac{-e^2 s \lambda}{2} \sin \theta$ | $\frac{-e^2 s \lambda}{2} \sin \theta$ | $\frac{-e^2 s \lambda}{2\sqrt{2}} (\tau' \cos \theta - 2\lambda)$ | $\frac{-e^2 s \lambda}{2\sqrt{2}} (\tau \cos \theta + 2\lambda)$ |
| T | $\frac{2\lambda - 1}{4t \sin^2 \theta_W}$ | $\cos \theta - \beta$ | $-\cos \theta - 2\tau\lambda$ | $\frac{s}{2m_W^2} \left[\cos \theta - \beta \left(1 + \frac{2m_W^2}{s} \right) \right]$ | $\frac{\sqrt{s}}{2m_W} \left[\cos \theta (1 + \beta^2) - 2\beta \right]$ $-\frac{2m_W \tau' \sin^2 \theta}{\sqrt{s} (\tau' \cos \theta - 2\lambda)}$ | $\frac{-\sqrt{s}}{2m_W} \left[\cos \theta (1 + \beta^2) - 2\beta \right]$ $+\frac{2m_W \tau \sin^2 \theta}{\sqrt{s} (\tau \cos \theta + 2\lambda)}$ |
| U | $\frac{2\lambda - 1}{4u \sin^2 \theta_W}$ | $\cos \theta + \beta$ | $-\cos \theta - 2\tau\lambda$ | $\frac{s}{2m_W^2} \left[\cos \theta + \beta \left(1 + \frac{2m_W^2}{s} \right) \right]$ | $\frac{\sqrt{s}}{2m_W} \left[\cos \theta (1 + \beta^2) + 2\beta \right]$ $-\frac{2m_W \tau' \sin^2 \theta}{\sqrt{s} (\tau' \cos \theta - 2\lambda)}$ | $\frac{-\sqrt{s}}{2m_W} \left[\cos \theta (1 + \beta^2) + 2\beta \right]$ $+\frac{2m_W \tau \sin^2 \theta}{\sqrt{s} (\tau \cos \theta + 2\lambda)}$ |
| G | $\frac{2Q_i}{s} (1 + \delta_\gamma) +$ $2(\cot \theta_w + \delta_Z) \frac{a_{Zi} - 2b_{Zi}\lambda}{s - m_Z^2}$ | $-\beta$ | 0 | $-\beta \left(1 + \frac{s}{2m_W^2} \right)$ | $-\beta \frac{\sqrt{s}}{m_W}$ | $\beta \frac{\sqrt{s}}{m_W}$ |
| X | $\frac{Q_i}{s} x_\gamma + x_Z \frac{a_{Zi} - 2b_{Zi}\lambda}{s - m_Z^2}$ | 0 | 0 | $-\beta \frac{s}{m_W^2}$ | $-\beta \frac{\sqrt{s}}{m_W}$ | $\beta \frac{\sqrt{s}}{m_W}$ |
| Y | $\frac{Q_i}{s} y_\gamma + y_Z \frac{a_{Zi} - 2b_{Zi}\lambda}{s - m_Z^2}$ | $-\beta \frac{s}{m_W^2}$ | 0 | 0 | $-\beta \frac{\sqrt{s}}{m_W}$ | $\beta \frac{\sqrt{s}}{m_W}$ |
| Z | $-\frac{Q_i}{s} z_\gamma - z_Z \frac{a_{Zi} - 2b_{Zi}\lambda}{s - m_Z^2}$ | 0 | 0 | 0 | $\beta^2 \tau' \left(\frac{\sqrt{s}}{m_W} \right)^3$ | $\beta^2 \tau \left(\frac{\sqrt{s}}{m_W} \right)^3$ |
| Z'_1 | $i \frac{Q_i}{s} z'_{1\gamma} + i z'_{1Z} \frac{a_{Zi} - 2b_{Zi}\lambda}{s - m_Z^2}$ | 0 | 0 | 0 | $-\beta \frac{\sqrt{s}}{m_W}$ | $-\beta \frac{\sqrt{s}}{m_W}$ |
| Z'_2 | $i \frac{Q_i}{s} z'_{2\gamma} + i z'_{2Z} \frac{a_{Zi} - 2b_{Zi}\lambda}{s - m_Z^2}$ | 2τ | 0 | 0 | $\tau' \frac{\sqrt{s}}{m_W}$ | $-\tau \frac{\sqrt{s}}{m_W}$ |
| Z'_3 | $-i \frac{Q_i}{s} z'_{3\gamma} - i z'_{3Z} \frac{a_{Zi} - 2b_{Zi}\lambda}{s - m_Z^2}$ | $2\tau \beta^2 \frac{s}{m_W^2}$ | 0 | 0 | 0 | 0 |

Table 3: Helicity Table for $W^\pm Z$ production. $\eta = \mp 1$ for W^\pm production.

| | | $\tau = \tau' = \pm 1$ | $\tau = -\tau' = \pm 1$ | $\tau = \tau' = 0$ | $\tau = 0, \tau' = \pm 1$ | $\tau = \pm 1, \tau' = 0$ |
|--------|---|---|---------------------------------------|--|---|--|
| | $\frac{1-2\lambda}{2\sqrt{2}\sin\theta_w} V_{ij}$ | $\frac{-e^2 s \lambda}{2} \sin\theta$ | $\frac{-e^2 s \lambda}{2} \sin\theta$ | $\frac{-e^2 s \lambda}{2} \sin\theta$ | $\frac{-e^2 s \lambda}{2\sqrt{2}} (\tau' \cos\theta - 2\lambda)$ | $\frac{-e^2 s \lambda}{2\sqrt{2}} (\tau \cos\theta + 2\lambda)$ |
| T | $+\eta \frac{a_{Zj} + b_{Zj}}{t}$ | $\frac{2\lambda\tau}{s} (m_Z^2 - m_W^2) + \cos\theta - \beta$ | $-\cos\theta - 2\lambda\tau$ | $\frac{s}{2m_Z m_W} \left[\cos\theta \left(1 - \frac{(m_Z^2 - m_W^2)^2}{s^2} \right) - \beta \left(1 + \frac{m_Z^2 + m_W^2}{s} \right) \right]$ | $\frac{\cos\theta (s - m_Z^2 - m_W^2) - s\beta}{m_Z \sqrt{s}} - \frac{2m_Z \tau' \sin^2\theta}{\sqrt{s} (\tau' \cos\theta - 2\lambda)}$ | $-\frac{\cos\theta (s - m_Z^2 - m_W^2) - s\beta}{m_W \sqrt{s}} + \frac{2m_W \tau \sin^2\theta}{\sqrt{s} (\tau \cos\theta + 2\lambda)}$ |
| U | $+\eta \frac{a_{Zi} + b_{Zi}}{u}$ | $\frac{2\lambda\tau}{s} (m_Z^2 - m_W^2) + \cos\theta + \beta$ | $-\cos\theta - 2\lambda\tau$ | $\frac{s}{2m_Z m_W} \left[\cos\theta \left(1 - \frac{(m_Z^2 - m_W^2)^2}{s^2} \right) + \beta \left(1 + \frac{m_Z^2 + m_W^2}{s} \right) \right]$ | $\frac{\cos\theta (s - m_Z^2 - m_W^2) + s\beta}{m_Z \sqrt{s}} - \frac{2m_Z \tau' \sin^2\theta}{\sqrt{s} (\tau' \cos\theta - 2\lambda)}$ | $-\frac{\cos\theta (s - m_Z^2 - m_W^2) + s\beta}{m_W \sqrt{s}} + \frac{2m_W \tau \sin^2\theta}{\sqrt{s} (\tau \cos\theta + 2\lambda)}$ |
| G | $\eta \frac{2(\cot\theta_w + \delta_Z)}{s - m_W^2}$ | $-\beta$ | 0 | $-\frac{\beta}{2m_Z m_W} (s + m_Z^2 + m_W^2)$ | $-\frac{\beta\sqrt{s}}{m_Z}$ | $\frac{\beta\sqrt{s}}{m_W}$ |
| X | $\eta \frac{x_Z}{s - m_W^2}$ | $-\beta$ | 0 | $-\beta \frac{m_Z}{m_W}$ | 0 | $\frac{\beta\sqrt{s}}{m_W}$ |
| Y | $\eta \frac{y_Z}{s - m_W^2}$ | $-\frac{s\beta}{m_W^2}$ | 0 | 0 | $-\beta\sqrt{s} \frac{m_Z}{m_W^2}$ | $\frac{\beta\sqrt{s}}{m_W}$ |
| Z | $\frac{z_Z}{s - m_W^2}$ | $-\frac{s\beta^2\tau}{m_W^2}$ | 0 | 0 | 0 | $\tau\beta^2 \left(\frac{\sqrt{s}}{m_W} \right)^3$ |
| Z'_1 | $-i \frac{z'_{1Z}}{s - m_W^2}$ | $-\beta$ | 0 | $\beta \frac{s - m_W^2}{m_Z m_W}$ | 0 | $-\frac{\beta\sqrt{s}}{m_W}$ |
| Z'_2 | $-i\eta \frac{z'_{2Z}}{s - m_W^2}$ | $+\frac{\tau}{s} (s - m_W^2 + m_Z^2)$ | 0 | 0 | $+\frac{2\tau t m_Z}{\sqrt{s}}$ | $\frac{-\tau}{m_W \sqrt{s}} (s - m_W^2 - m_Z^2)$ |
| Z'_3 | $-i\eta \frac{z'_{3Z}}{s - m_W^2}$ | 0 | 0 | 0 | $\frac{-2\tau t s \sqrt{s} \beta^2}{m_Z m_W^2}$ | 0 |

| | | $\tau = \tau' = \pm 1$ | $\tau = -\tau' = \pm 1$ | $\tau = \pm 1, \tau' = 0$ |
|--------|---|--|---------------------------------------|--|
| | $\frac{1-2\lambda}{2\sqrt{2}\sin\theta_w} V_{ij}$ | $\frac{-e^2 s \lambda}{2} \sin\theta$ | $\frac{-e^2 s \lambda}{2} \sin\theta$ | $\frac{-e^2 s \lambda}{2\sqrt{2}} (\tau \cos\theta + 2\lambda)$ |
| T | $\eta \frac{Q_j}{t}$ | $-2\lambda\tau \frac{m_W^2}{s} + \cos\theta - \beta$ | $-\cos\theta - 2\lambda\tau$ | $-\frac{2t}{m_W\sqrt{s}} + \frac{2m_W\tau \sin^2\theta}{\sqrt{s}(\tau \cos\theta + 2\lambda)}$ |
| U | $\eta \frac{Q_i}{u}$ | $-2\lambda\tau \frac{m_W^2}{s} + \cos\theta + \beta$ | $-\cos\theta - 2\lambda\tau$ | $\frac{2u}{m_W\sqrt{s}} + \frac{2m_W\tau \sin^2\theta}{\sqrt{s}(\tau \cos\theta + 2\lambda)}$ |
| G | $\eta 2(1 + \delta_\gamma)$ | $-\frac{1}{s}$ | 0 | $\frac{1}{m_W\sqrt{s}}$ |
| X | ηx_γ | $-\frac{1}{s}$ | 0 | $\frac{1}{m_W\sqrt{s}}$ |
| Y | ηy_γ | $-\frac{1}{m_W^2}$ | 0 | $\frac{1}{m_W\sqrt{s}}$ |
| Z | z_γ | $-\frac{\beta\tau}{m_W^2}$ | 0 | $\frac{\tau\sqrt{s}\beta}{m_W^3}$ |
| Z'_1 | $-i z'_{1\gamma}$ | $-\frac{1}{s}$ | 0 | $-\frac{1}{m_W\sqrt{s}}$ |
| Z'_2 | $-i\eta z'_{2\gamma}$ | $\frac{\tau}{s}$ | 0 | $-\frac{\tau}{m_W\sqrt{s}}$ |
| Z'_3 | $-i\eta z'_{3\gamma}$ | 0 | 0 | 0 |

Table 4: Helicity Table for $W^\pm\gamma$ production. $\eta = \mp 1$ for W^\pm production.

Table 5: Helicity Tables for ZZ, Z γ and $\gamma\gamma$ production.

| | | $\tau = \tau' = \pm 1$ | $\tau = -\tau' = \pm 1$ | $\tau = \tau' = 0$ | $\tau = 0, \tau' = \pm 1$ | $\tau = \pm 1, \tau' = 0$ |
|---|--|---|--|---|--|---|
| | 1 | $\frac{-e^2 s \lambda}{2} \sin \theta$ | $\frac{-e^2 s \lambda}{2} \sin \theta$ | $\frac{-e^2 s \lambda}{2} \sin \theta$ | $\frac{-e^2 s \lambda}{2\sqrt{2}} (\tau' \cos \theta - 2\lambda)$ | $\frac{-e^2 s \lambda}{2\sqrt{2}} (\tau \cos \theta + 2\lambda)$ |
| <u>For $\mathbf{q}_i^{(\prime)} \bar{\mathbf{q}}_i^{(\prime)} \rightarrow ZZ$ production:</u> | | | | | | |
| T | $\frac{4\lambda a_{Z_i} b_{Z_i} - a_{Z_i}^2 - b_{Z_i}^2}{t}$ | $\cos \theta - \beta$ | $-\cos \theta - 2\tau\lambda$ | $\frac{s}{2m_Z^2} \left[\cos \theta - \beta \left(1 + \frac{2m_Z^2}{s} \right) \right]$ | $\frac{\sqrt{s}}{2m_Z} \left[\cos \theta (1 + \beta^2) - 2\beta \right]$ $-\frac{2m_Z \tau' \sin^2 \theta}{\sqrt{s} (\tau' \cos \theta - 2\lambda)}$ | $\frac{-\sqrt{s}}{2m_Z} \left[\cos \theta (1 + \beta^2) - 2\beta \right]$ $+\frac{2m_Z \tau \sin^2 \theta}{\sqrt{s} (\tau \cos \theta + 2\lambda)}$ |
| U | $\frac{4\lambda a_{Z_i} b_{Z_i} - a_{Z_i}^2 - b_{Z_i}^2}{u}$ | $\cos \theta + \beta$ | $-\cos \theta - 2\tau\lambda$ | $\frac{s}{2m_Z^2} \left[\cos \theta + \beta \left(1 + \frac{2m_Z^2}{s} \right) \right]$ | $\frac{\sqrt{s}}{2m_Z} \left[\cos \theta (1 + \beta^2) + 2\beta \right]$ $-\frac{2m_Z \tau' \sin^2 \theta}{\sqrt{s} (\tau' \cos \theta - 2\lambda)}$ | $\frac{-\sqrt{s}}{2m_Z} \left[\cos \theta (1 + \beta^2) + 2\beta \right]$ $+\frac{2m_Z \tau \sin^2 \theta}{\sqrt{s} (\tau \cos \theta + 2\lambda)}$ |
| <u>For $\mathbf{q}_i^{(\prime)} \bar{\mathbf{q}}_i^{(\prime)} \rightarrow Z\gamma$ production:</u> | | | | | | |
| T | $Q_i \frac{2\lambda b_{Z_i} - a_{Z_i}}{t}$ | $-2\lambda\tau \frac{m_Z^2}{s} + \cos \theta - \beta$ | $-\cos \theta - 2\lambda\tau$ | | | $-\frac{2t}{m_Z \sqrt{s}} + \frac{2m_Z \tau \sin^2 \theta}{\sqrt{s} (\tau \cos \theta + 2\lambda)}$ |
| U | $Q_i \frac{2\lambda b_{Z_i} - a_{Z_i}}{u}$ | $-2\lambda\tau \frac{m_Z^2}{s} + \cos \theta + \beta$ | $-\cos \theta - 2\lambda\tau$ | | | $\frac{2u}{m_Z \sqrt{s}} + \frac{2m_Z \tau \sin^2 \theta}{\sqrt{s} (\tau \cos \theta + 2\lambda)}$ |
| <u>For $\mathbf{q}_i^{(\prime)} \bar{\mathbf{q}}_i^{(\prime)} \rightarrow \gamma\gamma$ production:</u> | | | | | | |
| T | $-\frac{2Q_i^2}{s}$ | 1 | $\frac{2\lambda\tau + \cos \theta}{1 - \cos \theta}$ | | | |
| U | $-\frac{2Q_i^2}{s}$ | -1 | $\frac{2\lambda\tau + \cos \theta}{1 + \cos \theta}$ | | | |

Standard part:

$$\begin{aligned}\mathcal{F}_{WW}^{T,T \text{ or } U,U} (1) &= 2a_T^2 \\ \mathcal{F}_{WW}^{G,G} (2) &= 4\mathcal{G}_{WW}^{V,V}(g_\gamma, g_\gamma, g_Z, g_Z) \\ \mathcal{F}_{WW}^{G,(T \text{ or } U)} (3) &= 2\mathcal{G}_{WW}^{V,(T \text{ or } U)}(g_\gamma, g_Z)\end{aligned}$$

CP conserving part:

$$\begin{aligned}\mathcal{F}_{WW}^{G,X} (4) &= 2\mathcal{G}_{WW}^{V,V}(g_\gamma, x_\gamma, g_Z, x_Z) \\ \mathcal{F}_{WW}^{G,Y} (5) &= 2\mathcal{G}_{WW}^{V,V}(g_\gamma, y_\gamma, g_Z, y_Z) \\ \mathcal{F}_{WW}^{GXY,Z} (6) &= \mathcal{G}_{WW}^{GXY,Z} \\ \mathcal{F}_{WW}^{X,(T \text{ or } U)} (7) &= \mathcal{G}_{WW}^{V,(T \text{ or } U)}(x_\gamma, x_Z) \\ \mathcal{F}_{WW}^{Y,(T \text{ or } U)} (8) &= \mathcal{G}_{WW}^{V,(T \text{ or } U)}(y_\gamma, y_Z) \\ \mathcal{F}_{WW}^{Z,(T \text{ or } U)} (9) &= \mathcal{G}_{WW}^{Z,(T \text{ or } U)} \\ \mathcal{F}_{WW}^{X,X} (10) &= \mathcal{G}_{WW}^{V,V}(x_\gamma, x_\gamma, x_Z, x_Z) \\ \mathcal{F}_{WW}^{Y,Y} (11) &= \mathcal{G}_{WW}^{V,V}(y_\gamma, y_\gamma, y_Z, y_Z) \\ \mathcal{F}_{WW}^{X,Y} (12) &= \mathcal{G}_{WW}^{V,V}(x_\gamma, y_\gamma, x_Z, y_Z) \\ \mathcal{F}_{WW}^{Z,Z} (13) &= \mathcal{G}_{WW}^{Z,Z}\end{aligned}$$

CP violating part:

$$\begin{aligned}\mathcal{F}_{WW}^{Z'_1,Z'_1} (14) &= a_\gamma^2 z'_{1\gamma}{}^2 + (a_Z^2 + b_Z^2)\chi_Z^2 z'_{1Z}{}^2 \\ &\quad + 2a_\gamma a_Z \chi_Z z'_{1\gamma} z'_{1Z} \\ \mathcal{F}_{WW}^{Z'_2,Z'_2} (15) &= a_\gamma^2 z'_{2\gamma}{}^2 + (a_Z^2 + b_Z^2)\chi_Z^2 z'_{2Z}{}^2 \\ &\quad + 2a_\gamma a_Z \chi_Z z'_{2\gamma} z'_{2Z} \\ \mathcal{F}_{WW}^{Z'_3,Z'_3} (16) &= a_\gamma^2 z'_{3\gamma}{}^2 + (a_Z^2 + b_Z^2)\chi_Z^2 z'_{3Z}{}^2 \\ &\quad + 2a_\gamma a_Z \chi_Z z'_{3\gamma} z'_{3Z} \\ \mathcal{F}_{WW}^{Z'_1,Z'_2} (17) &= -a_\gamma b_Z \chi_Z (z'_{1\gamma} z'_{2Z} + z'_{2\gamma} z'_{1Z}) \\ &\quad - 2a_Z b_Z \chi_Z^2 z'_{1Z} z'_{2Z} \\ \mathcal{F}_{WW}^{Z'_2,Z'_3} (18) &= a_\gamma^2 z'_{2\gamma} z'_{3\gamma} + (a_Z^2 + b_Z^2)\chi_Z^2 z'_{2Z} z'_{3Z} \\ &\quad + \chi_Z a_Z a_\gamma (z'_{2\gamma} z'_{3Z} + z'_{2Z} z'_{3\gamma})\end{aligned}$$

Table 6: $\mathcal{F}_{WW}^{\xi,\xi'}(i)$ coefficients for W^+W^- production.

$$\begin{aligned}
\mathcal{O}_{WW}^{T,T}(1) &= 4 \left\{ \frac{2s}{m_W^2} + \frac{s^2 \beta^2 \sin^2 \theta}{2} \left(\frac{1}{t^2} + \frac{1}{4m_W^4} \right) \right\} \\
\mathcal{O}_{WW}^{U,U}(1) &= 4 \left\{ \frac{2s}{m_W^2} + \frac{s^2 \beta^2 \sin^2 \theta}{2} \left(\frac{1}{u^2} + \frac{1}{4m_W^4} \right) \right\} \\
\mathcal{O}_{WW}^{G,G}(2) &= \frac{\beta^2}{8} \left\{ 16 \frac{s}{m_W^2} + \sin^2 \theta \left(\frac{s^2}{m_W^4} - \frac{4s}{m_W^2} + 12 \right) \right\} \\
\mathcal{O}_{WW}^{G,T}(3) &= 16 \left(1 + \frac{m_W^2}{t} \right) + 8\beta^2 \frac{s}{m_W^2} + \beta^2 \frac{\sin^2 \theta}{2} \left(\frac{s^2}{m_W^4} - \frac{2s}{m_W^2} - \frac{4s}{t} \right) \\
\mathcal{O}_{WW}^{G,U}(3) &= -16 \left(1 + \frac{m_W^2}{u} \right) - 8\beta^2 \frac{s}{m_W^2} - \beta^2 \frac{\sin^2 \theta}{2} \left(\frac{s^2}{m_W^4} - \frac{2s}{m_W^2} - \frac{4s}{u} \right)
\end{aligned}$$

Table 7: Standard $\mathcal{O}_{WW}^{\xi, \xi'}(i)$ coefficients for W^+W^- production.

$$\begin{aligned}
\mathcal{O}_{WW}^{G,X} (4) &= \frac{2|\vec{p}|^2}{m_W^4} \left\{ s + 6m_W^2 - \cos^2 \theta (s - 2m_W^2) \right\} \\
\mathcal{O}_{WW}^{G,Y} (5) &= \frac{16|\vec{p}|^2}{m_W^2} \\
\mathcal{O}_{WW}^{G,XY,Z} (6) &= \frac{32\sqrt{s}|\vec{p}|^3}{m_W^4} \cos \theta \\
\mathcal{O}_{WW}^{X,T} (7) &= \frac{|\vec{p}|\sqrt{s}}{tm_W^4} \left\{ -4|\vec{p}|^2 s \cos^3 \theta + 2|\vec{p}|\sqrt{s}(s - 2m_W^2) \cos^2 \theta \right. \\
&\quad \left. + (s^2 + 4sm_W^2 - 16m_W^4) \cos \theta - 2|\vec{p}|\sqrt{s}(s + 6m_W^2) \right\} \\
\mathcal{O}_{WW}^{X,U} (7) &= -\frac{|\vec{p}|\sqrt{s}}{um_W^4} \left\{ 4|\vec{p}|^2 s \cos^3 \theta + 2|\vec{p}|\sqrt{s}(s - 2m_W^2) \cos^2 \theta \right. \\
&\quad \left. - (s^2 + 4sm_W^2 - 16m_W^4) \cos \theta - 2|\vec{p}|\sqrt{s}(s + 6m_W^2) \right\} \\
\mathcal{O}_{WW}^{Y,T} (8) &= \frac{8}{tm_W^2} \left\{ |\vec{p}|\sqrt{s}(s - 2m_W^2) \cos \theta - 2s|\vec{p}|^2 \right\} \\
\mathcal{O}_{WW}^{Y,U} (8) &= -\frac{8}{um_W^2} \left\{ -|\vec{p}|\sqrt{s}(s - 2m_W^2) \cos \theta - 2s|\vec{p}|^2 \right\} \\
\mathcal{O}_{WW}^{Z,T} (9) &= \frac{16s|\vec{p}|^2}{m_W^4 t} \left\{ m_W^2 + 2\sqrt{s}|\vec{p}| \cos \theta - (s - m_W^2) \cos^2 \theta \right\} \\
\mathcal{O}_{WW}^{Z,U} (9) &= \frac{16s|\vec{p}|^2}{m_W^4 u} \left\{ m_W^2 - 2\sqrt{s}|\vec{p}| \cos \theta - (s - m_W^2) \cos^2 \theta \right\} \\
\mathcal{O}_{WW}^{X,X} (10) &= \frac{2|\vec{p}|^2}{m_W^4} \left\{ s + 2m_W^2 - \cos^2 \theta (s - 2m_W^2) \right\} \\
\mathcal{O}_{WW}^{Y,Y} (11) &= \frac{4|\vec{p}|^2}{m_W^4} \left\{ s + m_W^2 - \cos^2 \theta (s - m_W^2) \right\} \\
\mathcal{O}_{WW}^{X,Y} (12) &= \frac{8|\vec{p}|^2}{m_W^2} (1 + \cos^2 \theta) \\
\mathcal{O}_{WW}^{Z,Z} (13) &= \frac{16s|\vec{p}|^4}{m_W^6} (1 + \cos^2 \theta) \\
\mathcal{O}_{WW}^{Z'_1, Z'_1} (14) &= \frac{4|\vec{p}|^2}{m_W^2} (1 + \cos^2 \theta) \\
\mathcal{O}_{WW}^{Z'_2, Z'_2} (15) &= \frac{1}{m_W^2} \left\{ s(1 + \cos^2 \theta) + 4m_W^2 \sin^2 \theta \right\} \\
\mathcal{O}_{WW}^{Z'_3, Z'_3} (16) &= \frac{64|\vec{p}|^4}{m_W^4} \sin^2 \theta \\
\mathcal{O}_{WW}^{Z'_1, Z'_2} (17) &= \frac{8\sqrt{s}|\vec{p}|}{m_W^2} \cos \theta \\
\mathcal{O}_{WW}^{Z'_2, Z'_3} (18) &= -\frac{32|\vec{p}|^2}{m_W^2} (1 - \cos^2 \theta)
\end{aligned}$$

Table 8: Non standard $\mathcal{O}_{WW}^{\xi, \xi'}$ (i) coefficients for W^+W^- production.

| <u>Standard part:($V = Z$ or γ)</u> | |
|--|--|
| $\mathcal{F}_{WV}^{T,T}(1)$ | $= \mathcal{G}_{WV}^{T,T}$ |
| $\mathcal{F}_{WV}^{U,U}(2)$ | $= \mathcal{G}_{WV}^{U,U}$ |
| $\mathcal{F}_{WV}^{T,U}(3)$ | $= \mathcal{G}_{WV}^{T,U}$ |
| $\mathcal{F}_{WV}^{G,G}(4)$ | $= 4\mathcal{G}_{WV}^{V,V}(g_V, g_V)$ |
| $\mathcal{F}_{WV}^{G,T}(5)$ | $= 2\mathcal{G}_{WV}^{V,T}(g_V)$ |
| $\mathcal{F}_{WV}^{G,U}(6)$ | $= 2\mathcal{G}_{WV}^{V,U}(g_V)$ |
| <u>CP conserving part:</u> | |
| $\mathcal{F}_{WV}^{G,X}(7)$ | $= 2\mathcal{G}_{WV}^{V,V}(g_V, x_V)$ |
| $\mathcal{F}_{WV}^{G,Y}(8)$ | $= 2\mathcal{G}_{WV}^{V,V}(g_V, y_V)$ |
| $\mathcal{F}_{WV}^{GXY,Z}(9)$ | $= \mathcal{G}_{WV}^{GXY,Z}$ |
| $\mathcal{F}_{WV}^{X,T}(10)$ | $= \mathcal{G}_{WV}^{V,T}(x_V)$ |
| $\mathcal{F}_{WV}^{X,U}(11)$ | $= \mathcal{G}_{WV}^{V,U}(x_V)$ |
| $\mathcal{F}_{WV}^{Y,T}(12)$ | $= \mathcal{G}_{WV}^{V,T}(y_V)$ |
| $\mathcal{F}_{WV}^{Y,U}(13)$ | $= \mathcal{G}_{WV}^{V,U}(y_V)$ |
| $\mathcal{F}_{WV}^{Z,T}(14)$ | $= \mathcal{G}_{WV}^{Z,T}$ |
| $\mathcal{F}_{WV}^{Z,U}(15)$ | $= \mathcal{G}_{WV}^{Z,U}$ |
| $\mathcal{F}_{WV}^{X,X}(16)$ | $= \mathcal{G}_{WV}^{V,V}(x_V, x_V)$ |
| $\mathcal{F}_{WV}^{Y,Y}(17)$ | $= \mathcal{G}_{WV}^{V,V}(y_V, y_V)$ |
| $\mathcal{F}_{WV}^{X,Y}(18)$ | $= \mathcal{G}_{WV}^{V,V}(x_V, y_V)$ |
| $\mathcal{F}_{WV}^{Z,Z}(19)$ | $= \mathcal{G}_{WV}^{V,V}(z_V, z_V)$ |
| <u>CP violating part:</u> | |
| $\mathcal{F}_{WV}^{Z'_1, Z'_1}(20)$ | $= \mathcal{G}_{WV}^{V,V}(z'_{1V}, z'_{1V})$ |
| $\mathcal{F}_{WV}^{Z'_2, Z'_2}(21)$ | $= \mathcal{G}_{WV}^{V,V}(z'_{2V}, z'_{2V})$ |
| $\mathcal{F}_{WV}^{Z'_3, Z'_3}(22)$ | $= \mathcal{G}_{WV}^{V,V}(z'_{3V}, z'_{3V})$ |
| $\mathcal{F}_{WV}^{Z'_1, Z'_2}(23)$ | $= \mathcal{G}_{WV}^{V,V}(z'_{1V}, z'_{2V})$ |
| $\mathcal{F}_{WV}^{Z'_2, Z'_3}(24)$ | $= \mathcal{G}_{WV}^{V,V}(z'_{2V}, z'_{3V})$ |

Table 9: $\mathcal{F}_{WV}^{\xi, \xi'}(i)$ coefficients for $W^\pm Z$ and $W^\pm \gamma$ production.

$$\begin{aligned}
\mathcal{O}_{WZ}^{T,T}(1) &= 8 \left\{ \frac{s}{m_W^2} + \frac{s}{m_Z^2} + (ut - m_W^2 m_Z^2) \left(\frac{2}{t^2} + \frac{1}{2m_W^2 m_Z^2} \right) \right\} \\
\mathcal{O}_{WZ}^{U,U}(2) &= 8 \left\{ \frac{s}{m_W^2} + \frac{s}{m_Z^2} + (ut - m_W^2 m_Z^2) \left(\frac{2}{u^2} + \frac{1}{2m_W^2 m_Z^2} \right) \right\} \\
\mathcal{O}_{WZ}^{T,U}(3) &= 16 \left\{ \frac{2s(m_W^2 + m_Z^2)}{ut} - \frac{s(m_W^2 + m_Z^2)}{m_W^2 m_Z^2} - \frac{ut - m_W^2 m_Z^2}{2m_W^2 m_Z^2} \right\} \\
\mathcal{O}_{WZ}^{G,G}(4) &= 2 \left\{ (ut - m_W^2 m_Z^2) \left[4 + \frac{(s - m_W^2 - m_Z^2)^2}{2m_W^2 m_Z^2} \right] \right. \\
&\quad \left. + s \frac{m_W^2 + m_Z^2}{m_W^2 m_Z^2} \left[(s - m_W^2 - m_Z^2)^2 - 4m_W^2 m_Z^2 \right] \right\} \\
\mathcal{O}_{WZ}^{G,T}(5) &= -\frac{8}{t} \left\{ 2s(m_W^2 + m_Z^2) \left(1 + t \frac{s - m_W^2 - m_Z^2}{2m_W^2 m_Z^2} \right) \right. \\
&\quad \left. + (m_W^2 m_Z^2 - ut) \left(2 - t \frac{s - m_W^2 - m_Z^2}{2m_W^2 m_Z^2} \right) \right\} \\
\mathcal{O}_{WZ}^{G,U}(6) &= \frac{8}{u} \left\{ 2s(m_W^2 + m_Z^2) \left(1 + u \frac{s - m_W^2 - m_Z^2}{2m_W^2 m_Z^2} \right) \right. \\
&\quad \left. + (m_W^2 m_Z^2 - ut) \left(2 - u \frac{s - m_W^2 - m_Z^2}{2m_W^2 m_Z^2} \right) \right\}
\end{aligned}$$

Table 10: Standard $\mathcal{O}_{WZ}^{\xi,\xi'}(i)$ coefficients for $W^\pm Z$ production.

$$\begin{aligned}
\mathcal{O}_{WZ}^{G,X} (7) &= \frac{4s|\vec{p}|^2}{m_W^2} \left\{ 4s + (5m_W^2 + m_Z^2 - s) \sin^2 \theta \right\} \\
\mathcal{O}_{WZ}^{G,Y} (8) &= \frac{32s^2|\vec{p}|^2}{m_W^2} \\
\mathcal{O}_{WZ}^{GXY,Z} (9) &= \eta \frac{64s^2|\vec{p}|^4}{\beta m_W^4} \cos \theta \\
\mathcal{O}_{WZ}^{X,T} (10) &= \frac{8s|\vec{p}|^2}{\beta t m_W^2} \left\{ 2 \cos \theta (m_W^2 + m_Z^2 - s) + 2s\beta + \beta \sin^2 \theta (t + 2m_W^2) \right\} \\
\mathcal{O}_{WZ}^{X,U} (11) &= \frac{8s|\vec{p}|^2}{\beta u m_W^2} \left\{ 2 \cos \theta (m_W^2 + m_Z^2 - s) - 2s\beta - \beta \sin^2 \theta (u + 2m_W^2) \right\} \\
\mathcal{O}_{WZ}^{Y,T} (12) &= \frac{32s|\vec{p}|^2}{\beta t m_W^2} (2t \cos \theta + s\beta \sin^2 \theta) \\
\mathcal{O}_{WZ}^{Y,U} (13) &= \frac{32s|\vec{p}|^2}{\beta u m_W^2} (2u \cos \theta - s\beta \sin^2 \theta) \\
\mathcal{O}_{WZ}^{Z,T} (14) &= -\eta \frac{16s|\vec{p}|^2}{m_W^4 t} \left\{ m_W^2 [(m_Z^2 - m_W^2) \sin^2 \theta - s] + s \cos \theta [(s - m_Z^2) \cos \theta - s\beta] \right\} \\
\mathcal{O}_{WZ}^{Z,U} (15) &= -\eta \frac{16s|\vec{p}|^2}{m_W^4 u} \left\{ m_W^2 [(m_Z^2 - m_W^2) \sin^2 \theta - s] + s \cos \theta [(s - m_Z^2) \cos \theta + s\beta] \right\} \\
\mathcal{O}_{WZ}^{X,X} (16) &= \frac{4s|\vec{p}|^2}{m_W^2} \left\{ 2s + (2m_W^2 + m_Z^2 - s) \sin^2 \theta \right\} \\
\mathcal{O}_{WZ}^{Y,Y} (17) &= \frac{4s^2|\vec{p}|^2}{m_W^4} \left\{ 4s + (m_W^2 + m_Z^2 - 2s)(1 + \cos^2 \theta) \right\} \\
\mathcal{O}_{WZ}^{X,Y} (18) &= \frac{8s^2|\vec{p}|^2}{m_W^2} (3 - \cos^2 \theta) \\
\mathcal{O}_{WZ}^{Z,Z} (19) &= \frac{16s^2|\vec{p}|^4}{m_W^6} \left\{ 4m_W^2 + (s - 2m_W^2)(1 + \cos^2 \theta) \right\} \\
\mathcal{O}_{WZ}^{Z'_1,Z'_1} (20) &= \frac{4s|\vec{p}|^2}{m_W^2 m_Z^2} \left\{ [(m_W^2 + m_Z^2 - s)^2 - m_Z^4 + s m_Z^2] \sin^2 \theta + 2s m_Z^2 \right\} \\
\mathcal{O}_{WZ}^{Z'_2,Z'_2} (21) &= \frac{1}{m_W^2} \left\{ (m_W^2 - m_Z^2)^2 (2m_W^2 - 4s) + s [(m_W^2 + m_Z^2)^2 + (s - m_Z^2)^2 + 3m_Z^4] \right. \\
&\quad \left. + s^2 \beta^2 \cos^2 \theta (s - 2m_W^2) \right\} \\
\mathcal{O}_{WZ}^{Z'_3,Z'_3} (22) &= \frac{64s^3|\vec{p}|^4}{m_W^4 m_Z^2} (1 + \cos^2 \theta) \\
\mathcal{O}_{WZ}^{Z'_1,Z'_2} (23) &= -\eta \frac{16s|\vec{p}|^2}{\beta m_W^2} \cos \theta (s - m_W^2 - m_Z^2) \\
\mathcal{O}_{WZ}^{Z'_2,Z'_3} (24) &= -\frac{32s^2|\vec{p}|^2}{m_W^2} (1 + \cos^2 \theta)
\end{aligned}$$

Table 11: Non standard $\mathcal{O}_{WZ}^{\xi,\xi'}(i)$ coefficients for $W^\pm Z$ production.

$$\begin{aligned}
\mathcal{O}_{W\gamma}^{T,T}(1) &= \frac{8}{s^2 \beta^2 m_W^2 t} \left\{ 2m_W^2 (um_W^4 - s^2 t - s^3 \beta) + st(t^2 + u^2) \right\} \\
\mathcal{O}_{W\gamma}^{U,U}(2) &= \frac{8}{s^2 \beta^2 m_W^2 u} \left\{ 2m_W^2 (tm_W^4 - s^2 u - s^3 \beta) + su(t^2 + u^2) \right\} \\
\mathcal{O}_{W\gamma}^{T,U}(3) &= -\frac{16}{s \beta^2 m_W^2} (t^2 + u^2 - 4m_W^4) \\
\mathcal{O}_{W\gamma}^{G,G}(4) &= \frac{2s}{m_W^2} (u^2 + t^2) + 8ut \\
\mathcal{O}_{W\gamma}^{G,T}(5) &= \frac{8}{m_W^2} \left\{ 2m_W^2 u + s(u - t \cos \theta) \right\} \\
\mathcal{O}_{W\gamma}^{G,U}(6) &= -\frac{8}{m_W^2} \left\{ 2m_W^2 t + s(t + u \cos \theta) \right\}
\end{aligned}$$

Table 12: Standard $\mathcal{O}_{W\gamma}^{\xi, \xi'}(i)$ coefficients for $W^\pm \gamma$ production.

$$\begin{aligned}
\mathcal{O}_{W\gamma}^{G,X} (7) &= 16ut + \frac{4s}{m_W^2}(t^2 + u^2) \\
\mathcal{O}_{W\gamma}^{G,Y} (8) &= \frac{4s}{m_W^2} \{2ut + s^2\beta^2\} \\
\mathcal{O}_{W\gamma}^{G,XY,Z} (9) &= \eta \frac{4s^4\beta^3}{m_W^4} \cos\theta \\
\mathcal{O}_{W\gamma}^{X,T} (10) &= -\frac{8}{\beta m_W^2} \{t^2 + u^2 - 2\beta m_W^2 u\} \\
\mathcal{O}_{W\gamma}^{X,U} (11) &= \frac{8}{\beta m_W^2} \{t^2 + u^2 - 2\beta m_W^2 t\} \\
\mathcal{O}_{W\gamma}^{Y,T} (12) &= -\frac{8}{\beta m_W^2} \{2ut + s^2\beta^2\} \\
\mathcal{O}_{W\gamma}^{Y,U} (13) &= \frac{8}{\beta m_W^2} \{2ut + s^2\beta^2\} \\
\mathcal{O}_{W\gamma}^{Z,T} (14) &= \eta \frac{8}{m_W^4} \{s^3\beta^2 + 2(s^2 + m_W^4)u\} \\
\mathcal{O}_{W\gamma}^{Z,U} (15) &= \eta \frac{8}{m_W^4} \{s^3\beta^2 + 2(s^2 + m_W^4)t\} \\
\mathcal{O}_{W\gamma}^{X,X} (16) &= \frac{2}{m_W^2} \{4utm_W^2 + s(t^2 + u^2)\} \\
\mathcal{O}_{W\gamma}^{Y,Y} (17) &= \frac{2s}{m_W^4} \{4uts + m_W^2(t^2 + u^2)\} \\
\mathcal{O}_{W\gamma}^{X,Y} (18) &= \frac{4s}{m_W^2} \{2ut + s^2\beta^2\} \\
\mathcal{O}_{W\gamma}^{Z,Z} (19) &= \frac{2s^2\beta^2}{m_W^6} \{4utm_W^2 + s(t^2 + u^2)\} \\
\mathcal{O}_{W\gamma}^{Z'_1,Z'_1} (20) &= \frac{2}{m_W^2} \{4utm_W^2 + s(t^2 + u^2)\} \\
\mathcal{O}_{W\gamma}^{Z'_2,Z'_2} (21) &= \frac{2}{m_W^2} \{4utm_W^2 + s(t^2 + u^2)\} \\
\mathcal{O}_{W\gamma}^{Z'_3,Z'_3} (22) &= 0 \\
\mathcal{O}_{W\gamma}^{Z'_1,Z'_2} (23) &= \eta \frac{4s^3\beta^2}{m_W^2} \cos\theta
\end{aligned}$$

Table 13: Non standard $\mathcal{O}_{W\gamma}^{\xi,\xi'}(i)$ coefficients for $W^\pm\gamma$ production.

| |
|--|
| $\mathcal{O}_{ZZ}^{T,T}(1) = 4 \left\{ \frac{2s}{m_Z^2} + \frac{s^2 \beta^2 \sin^2 \theta}{2} \left(\frac{1}{t^2} + \frac{1}{4m_Z^4} \right) \right\}$ $\mathcal{O}_{ZZ}^{U,U}(2) = 4 \left\{ \frac{2s}{m_Z^2} + \frac{s^2 \beta^2 \sin^2 \theta}{2} \left(\frac{1}{u^2} + \frac{1}{4m_Z^4} \right) \right\}$ $\mathcal{O}_{ZZ}^{T,U}(3) = 8 \left\{ \frac{4sm_Z^2}{ut} - \frac{2s}{m_Z^2} - \frac{ut - m_Z^4}{2m_Z^4} \right\}$ |
| <hr/> $\mathcal{O}_{Z\gamma}^{T,T}(1) = \frac{4}{s^2 \beta^2 m_Z^2 t} \left\{ 2m_Z^2 (um_Z^4 - s^2 t - s^3 \beta) + st(t^2 + u^2) \right\}$ $\mathcal{O}_{Z\gamma}^{U,U}(2) = \frac{4}{s^2 \beta^2 m_Z^2 u} \left\{ 2m_Z^2 (tm_Z^4 - s^2 u - s^3 \beta) + su(t^2 + u^2) \right\}$ $\mathcal{O}_{Z\gamma}^{T,U}(3) = -\frac{8}{s \beta^2 m_Z^2} (t^2 + u^2 - 4m_Z^4)$ |
| <hr/> $\mathcal{O}_{\gamma\gamma}^{T,T}(1) = -\frac{4s}{t} (1 + \cos^3 \theta)$ $\mathcal{O}_{\gamma\gamma}^{U,U}(2) = -\frac{4s}{u} (1 - \cos^3 \theta)$ $\mathcal{O}_{\gamma\gamma}^{T,U}(3) = 16 \cos^2 \theta$ |
| <hr/> $\mathcal{F}_{VV'}^{T,T}(1) = \mathcal{F}_{VV'}^{U,U}(2) = \mathcal{F}_{VV'}^{T,U}(3) = \mathcal{F}_{VV'}$ $\mathcal{F}_{ZZ} = 4a_{Z_i}^2 b_{Z_i}^2 + (a_{Z_i}^2 + b_{Z_i}^2)^2$ $\mathcal{F}_{Z\gamma} = Q_i^2 (a_{Z_i}^2 + b_{Z_i}^2)$ $\mathcal{F}_{\gamma\gamma} = Q_i^4$ |

Table 14: Standard $\mathcal{O}_{VV'}^{\xi_i, \xi'_i}(i)$ and $\mathcal{F}_{VV'}^{\xi_i, \xi'_i}(i)$ coefficients for $\mathbf{q}_i^{(\prime)} \bar{\mathbf{q}}_i^{(\prime)} \rightarrow \mathbf{V}\mathbf{V}'$ with $VV' = ZZ, Z\gamma, \gamma\gamma$.